Geochemistry Geophysics Geosystems G3

Article
Volume 12, Number 12
9 December 2011
Q12008, doi:10.1029/2011GC003853
ISSN: 1525-2027

Published by AGU and the Geochemical Society

Seismogenic characteristics of the Northern Mariana shallow thrust zone from local array data

Erica L. Emry and Douglas A. Wiens
Department of Earth and Planetary Sciences, Washington University in St. Louis, Campus Box 1169, One Brookings Drive, St. Louis, Missouri 63130-4899, USA (ericae@seismo.wustl.edu)

Hajime Shiobara
Earthquake Research Institute, University of Tokyo, 1-1-1 Yayoi, Bunkyo-ku, Tokyo 113-0032, Japan

Hiroko Sugioka
Institute for Frontier Research on Earth Evolution, JAMSTEC, 2-15 Natsushima-Cho, Yokosuka-city, Yokosuka 237-0061, Japan

[1] The Northern Mariana seismogenic zone has no shallow thrust earthquakes larger than Ms 7.4 in the historical seismological record and is traditionally considered 'decoupled' or 'aseismic'. During the 2003–2004 Mariana Subduction Factory Imaging Experiment, we recorded local shallow earthquakes throughout the central and northern regions of the Mariana forearc using an array of terrestrial broadband and ocean bottom seismographs. Accurate locations for both the 2003–2004 local seismicity as well as earthquakes with Global Centroid Moment Tensor (GCMT) solutions from 1976 to 2008 were obtained using the hypocentroidal decomposition relocation method and a local velocity model. Additionally, focal mechanisms for the largest 2003–2004 earthquakes were determined using regional waveform inversion. Thrust faulting earthquakes occur along the Mariana megathrust between depths of 20–60 km, showing that the lack of great shallow thrust earthquakes does not result from a narrow seismogenic zone and that most seismicity occurs where the downgoing plate contacts the overriding mantle wedge. Clusters of small plate interface earthquakes with Ml 1.6–4.7 occur within patches 100–120 km west of the trench at depths of 30–45 km. Furthermore, the larger GCMT earthquakes (Mw 4.9–5.8) occur mostly updip and downdip of the patches of smaller earthquakes recorded by our local array and is suggestive of changes in the fault properties with depth. Clusters of small, forearc earthquakes occur discontinuously along the length of the Mariana subduction zone, showing that Northern Mariana is variable both along the strike of the margin and with depth along the seismogenic zone. We propose that the lack of great (Mw > 8) thrust faulting earthquakes is due in part to the variable frictional heterogeneity along the megathrust.

Components: 13,900 words, 9 figures, 3 tables.

Keywords: Northern Mariana; seismogenic zone; shallow thrust seismicity.

Index Terms: 7215 Seismology: Earthquake source observations (1240); 7230 Seismology: Seismicity and tectonics (1207, 1217, 1240, 1242); 8170 Tectonophysics: Subduction zone processes (1031, 3060, 3613, 8413).

Received 30 August 2011; **Revised** 24 October 2011; **Accepted** 26 October 2011; **Published** 9 December 2011.

Emry, E. L., D. A. Wiens, H. Shiobara, and H. Sugioka (2011), Seismogenic characteristics of the Northern Mariana shallow thrust zone from local array data, *Geochem. Geophys. Geosyst.*, *12*, Q12008, doi:10.1029/2011GC003853.

1. Introduction

[2] The Mariana subduction zone is commonly considered to be the aseismic end-member on a spectrum of subduction zones, with the opposite end represented by the Chilean and Alaskan margins, where megathrust earthquakes approaching Mw 9.5 are feasible [*Kanamori*, 1977; *Uyeda and Kanamori*, 1979]. To date, no great (Mw > 8.0) shallow thrust earthquakes have been recorded and accurately located in the Mariana subduction zone, although historical records do contain evidence for infrequent moderate-sized (Mw > 7.0) shallow events and large earthquakes for which magnitude estimates are absent or unreliable (Table 1). In a global study comparing seismic slip coefficients, the Mariana Islands was determined to have a seismic coupling coefficient of 0.002, meaning that only 0.2% of the slip between the Pacific and Philippine plates could be accounted for by historical records of large thrust earthquakes [*Pacheco et al.*, 1993]. The results imply that either a large percentage of interplate slip is accommodated through stable, aseismic slip or that the subduction zone is due for a giant earthquake every hundred years.

[3] Recent devastating magnitude nine earthquakes in regions previously thought to have little potential for great earthquakes have caused reassessment of such seismic/aseismic classifications. Sumatra, for example, had a coupling coefficient of 0.007 determined by *Pacheco et al.* [1993], yet produced a Mw ~9.1 earthquake in 2004 [e.g., *Lay et al.*, 2005]. The recent 2011 Northeast Japan earthquake also occurred in a region where magnitude nine earthquakes were thought to be impossible. Clearly a much better understanding of the factors controlling the seismic characteristics of the subduction zone thrust interface is needed.

[4] Previous studies present two main hypotheses to explain the lack of large earthquakes in the Mariana and other 'aseismic' subduction zones. The first suggests that the shallow intersection of the plate interface with a serpentinized mantle wedge narrows the seismogenic width so that large earthquakes are not possible [*Hyndman et al.*, 1997; *Peacock and Hyndman*, 1999; *Hyndman*, 2007]. This idea proposes that seismic slip is limited to where the underthrusting plate contacts the overriding forearc crust, which occurs in the Central and Northern Mariana Islands at a depth of about 15 km [*Takahashi et al.*, 2007]. The second hypothesis for lack of large earthquakes in Mariana is that the plate interface is very weakly coupled due to the geometry of the subduction zone and predominance of horizontal tensional tectonic stresses in the region, as evidenced by seafloor spreading in the back arc [*Scholz and Campos*, 1995].

[5] In the absence of large underthrusting earthquakes, the depth extent of the seismogenic zone may be identified through use of microseismicity or by geodesy [*Schwartz and DeShon*, 2007]. Seismic studies are the most feasible option in an island arc setting, given that the geodetic signal of plate coupling and strain accumulation occurs offshore, where geodetic studies require extremely expensive ocean-bottom GPS technology. Through seismic studies, we can examine the pattern of seismic release along the thrust zone and obtain a rough estimate of how much surface area could rupture seismically if it were all to slip at once.

[6] In this paper we use shallow earthquake locations and focal mechanisms for small earthquakes recorded by a temporary local array of land and ocean bottom seismographs deployed during 2003–2004 to better understand the Northern Mariana shallow thrust region [*Pozgay et al.*, 2007]. Previously, the Northern Mariana subduction zone had only been studied using larger earthquakes detectable teleseismically, since there are few permanent seismic stations in this region. The local recordings provide for study of much smaller earthquakes with much greater location precision, allowing us to answer basic questions about the characteristics of this unusual subduction zone.

2. Background

2.1. Geological Setting

2.1.1. Tectonic Setting and History

[7] The Mariana-Izu-Bonin system is a young subduction zone extending from Japan in the north to Guam in the south that first formed about 43 Ma [*Stern et al.*, 2003]. The Mariana Islands are the southern portion of the island chain, where a strong, outward curvature of the arc separates it from the mostly North-South Izu-Bonin section. Throughout the history of the Mariana Islands, the volcanic arc has split twice – the remnant arcs from these rifting events constitute the Kyushu-Palau ridge and the West Mariana Ridge [*Stern et al.*, 2003]. Evidence from paleomagnetism suggests the orientation of the Izu-Bonin-Mariana system was originally East-West and gradually rotated clockwise to its current North-South orientation [*Hall et al.*, 1995; *Hall*, 2002]. The convergence rate between the Pacific plate and the forearc of the Mariana subduction

Table 1. Large Shallow Earthquakes (M ≥ 7 or Guam MMI ≥ 8) in the Mariana Forearc 1825–2011

Event	Date	Time (UTC)	Latitude (°N)	Longitude (°E)	Depth (km)	Type of Slip	Magnitude and/or Intensity
1	Apr 1825	n/a	n/a[a]	n/a[a]	n/a	n/a	8 MMI[b]
2	May 1834	n/a	n/a[a]	n/a[a]	n/a	n/a	8 MMI[b]
3	25 Jan 1849	14:56[b,c]	n/a[a]	n/a[a]	n/a	n/a	M 7.5[d]/9 MMI[b]
4	16 May 1892	21:10[b,c]	n/a[a]	n/a[a]	n/a	n/a	M 7.5[d]/8 MMI[b]
5	22 Sept 1902	1:46:30[e]	18.0[e]	146.0[e]	n/a	n/a	Ms 7.4[f]/9 MMI[b]
6	23 Mar 1913	20:47.3	24[g]	142[g]	80[g]	n/a	mb 7.1[h]
7	24 Oct 1930	20:15:11	18.5[g]	147[g]	35[g]	n/a	Ms 7.0[h]
8	28 Jan 1931	21:24:03	11[g]	144.75[g]	35[g]	n/a	Ms 7.1[h]
9	24 Feb 1934	6:23:40	22.5[g]	144[g]	35[g]	n/a	Ms 7.1[f]
10	17 Jan 1940	01:15:00	17[g]	148[g]	80[g]	n/a	mb 7.3[i]
11	28 Dec 1940	16:37:44	18[e]	147.5[g]	80[g]	n/a	mb 7.3[i]
12	14 Jun 1942	03:09:45	15[g]	145[g]	80[g]	n/a	mb 7.0[h]
13	25 May 1950	18:35:07	13[g]	143.5[g]	90[g]	n/a	mb 7.0[h]
14[j]	8 Aug 1993	8:34:49.3	13.06	145.31	59.3	Thrust	Mw 7.7
15[j]	12 Oct 2001	15:02:23.3	12.88	145.08	42.0	Thrust	Mw 7.0
16[j]	26 Apr 2002	16:06:13.9	13.15	144.67	69.1	Thrust	Mw 7.0

[a]Strong shaking felt on island of Guam, earthquake locations unknown.
[b]*Maso* [1910].
[c]Indicates Local Guam Time.
[d]*Soloviev and Go* [1974].
[e]*Gutenberg* [1956].
[f]*Pacheco and Sykes* [1992].
[g]*Gutenberg and Richter* [1954].
[h]*Abe* [1981].
[i]*Abe and Kanamori* [1979].
[j]Global GCMT catalog, *Dziewonski et al.* [1981].

zone from GPS measurements at stations along the island arc and forearc rise show that the arc and forearc are moving east relative to the rest of the Philippine Sea plate, due to active extension in the back-arc basin [*Kato et al.*, 2003]. The rate of subduction beneath the northern part of the Mariana Islands near Agrihan is 35–45 mm/yr, while the rate of subduction in the south near Guam is 60–70 mm/yr [*Kato et al.*, 2003]. The angle of convergence of the Pacific plate beneath the Mariana forearc is 83° West of North (Figure 1) [*Kato et al.*, 2003].

2.1.2. Forearc Morphology

[8] The western portion of the forearc in our study region is flat, covered in volcaniclastic and pelagic sediments, and spans about 2/3 of the forearc seafloor. The region is cut by normal faults that run roughly parallel to the trend of the volcanic arc and the trench, the presence of which indicate that the Mariana forearc is under tension [*Stern and Smoot*, 1998]. The eastern portion of the forearc is cut by numerous, small normal faults in a mostly southwest to northeast orientation [*Stern and Smoot*, 1998]. In this highly deformed part of the forearc, a number of large serpentinite seamounts, unique to the Izu-Bonin-Mariana subduction zone are present [*Stern et al.*, 2003]. The serpentinite seamounts in the Mariana forearc are located at 15–90 km distance from the trench and are formed through serpenitite mud volcanism. The minerals ejected reflect increasing pressure as distance from the trench increases, suggesting that materials are being ejected from progressively deeper depths [*Fryer and Salisbury*, 2006]. The Big Blue seamount is located at 70 km to the west of the trench [*Oakley et al.*, 2007] and is the largest seamount located on the Mariana forearc. The tectonic instability of the Mariana forearc is responsible for the presence of the active serpentinite seamounts, as fluids expelled during subduction are able to move upward through the extensively faulted forearc and erupt at the surface [*Fryer et al.*, 1999; *Stern et al.*, 2003; *Fryer and Salisbury*, 2006].

[9] The presence of serpentinite mud volcanoes is frequently used as evidence that the underlying Mariana mantle wedge is serpentinized. Geochemical work from *Benton et al.* [2004] found that expelled fluids were not derived directly from the slab, but rather, had interacted with mantle wedge materials prior to being emitted from the seamount. Receiver functions calculated beneath Saipan and Tinian Islands further to the south reveal a pronounced low velocity layer in the mantle wedge at 40–55 km depth, leading to the conclusion that mantle serpentinization is prevalent at these depths [*Tibi et al.*, 2008]. *Pozgay et al.* [2009] suggest mantle serpentinization in the forearc beneath the seamounts as an explanation for an observed zone

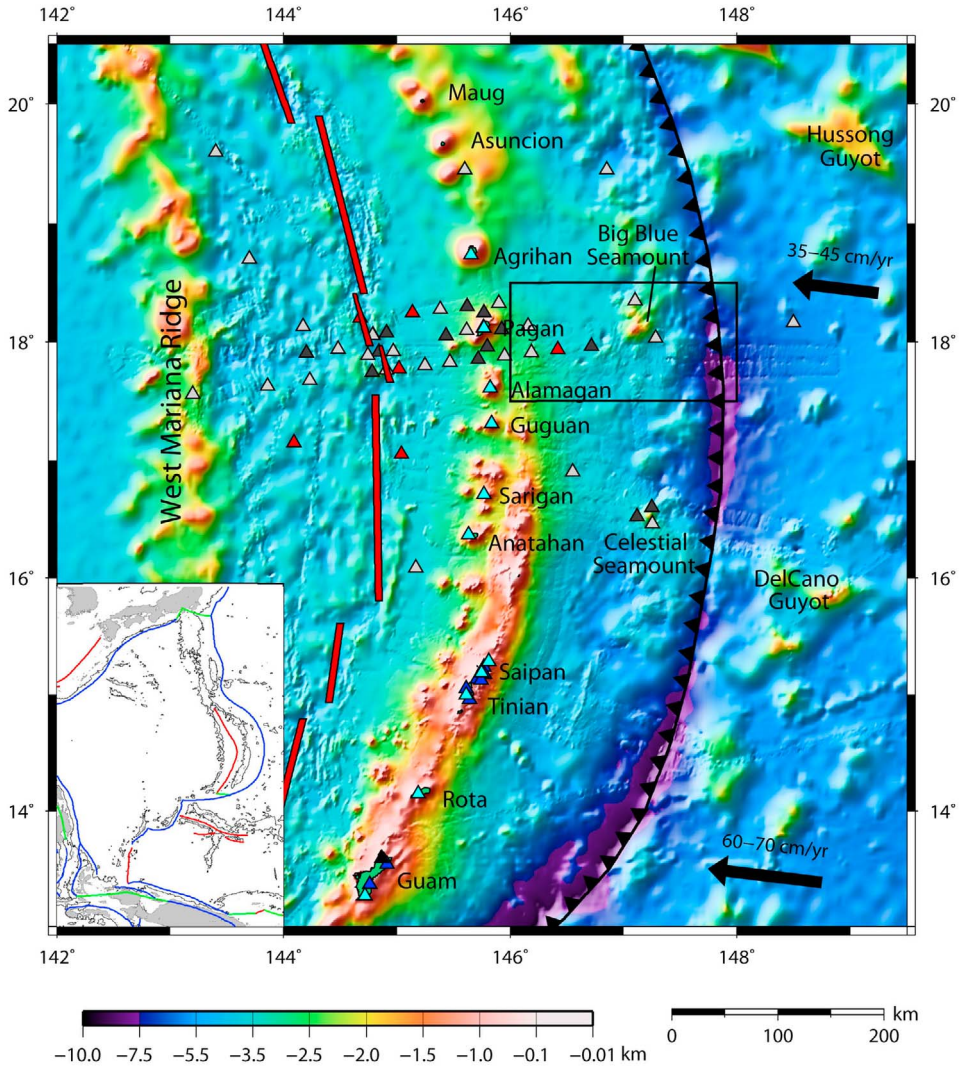
142°
144°
146°
148°
20°
18°
16°
14°
Maug
Asuncion
Hussong Guyot
Big Blue Seamount
Agrihan
35–45 cm/yr
West Mariana Ridge
Pagan
Alamagan
Guguan
Sarigan
Anatahan
Celestial Seamount
DelCano Guyot
Saipan
Tinian
Rota
Guam
60–70 cm/yr
−10.0 −7.5 −5.5 −3.5 −2.5 −2.0 −1.5 −1.0 −0.1 −0.01 km
km
0 100 200

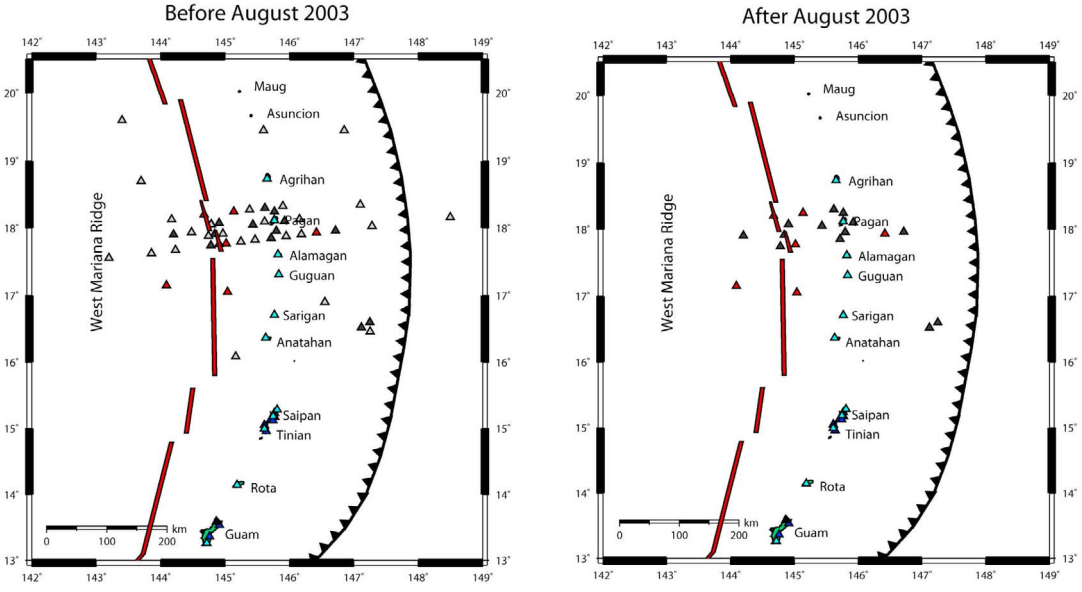
Before August 2003
After August 2003
West Mariana Ridge
Maug
Asuncion
Agrihan
Pagan
Alamagan
Guguan
Sarigan
Anatahan
Saipan
Tinian
Rota
Guam
km
0 100 200

Figure 1

of high attenuation. Results from surface wave phase velocities in the Northern Mariana Islands also showed a low velocity anomaly in the forearc between Celestial and Big Blue Seamounts [*Pyle et al.*, 2010], postulated to be mantle serpentinization. Similarly, P and S velocity tomography by *Barklage* [2010] revealed a region of an unusually high 1.95–2.0 Vp/Vs ratio; this combined with modeling by *Hacker et al.* [2003] suggests that the forearc mantle wedge is ~30–60% serpentinized. While the evidence for a serpentinized mantle wedge in Mariana is substantial, its spatial distribution is not well constrained and its relation to shallow forearc seismicity is not completely understood.

2.2. Seismicity

[10] The most recent, large, shallow thrust earthquakes have occurred in the Southern Mariana Islands near Guam (Figure 2 and Table 1, events 14–16) and began with a Mw 7.7 earthquake on August 8, 1993 [*Campos et al.*, 1996]. Depth estimates for this earthquake vary from 41.5 km [*Campos et al.*, 1996] to 74.5 km [*Harada and Ishibashi*, 2008], and the focal mechanism is consistent with a shallow dipping thrust earthquake [*Campos et al.*, 1996]. In 2001 and 2002, two large Mw 7.0 earthquakes occurred nearby the location of the large 1993 earthquake. The large 1993 Guam earthquake was initially interpreted as rupture along the plate interface [*Campos et al.*, 1996] and supported the interpretation that the Southern Mariana plate interface is more strongly coupled than the Northern plate interface [*Scholz and Campos*, 1995]. However, more recent studies suggest that 1993, 2001, and 2002 Guam earthquakes occurred in the subducting Pacific plate and thus do not represent seismic slip along the megathrust [*Tanioka et al.*, 1995; *Harada and Ishibashi*, 2008].

[11] A number of potentially shallow thrust earthquakes with magnitudes greater than 7.0 occurred from 1900 to 1950. Many of these events, listed by *Gutenberg and Richter* [1954] as shallow or intermediate depth earthquakes, have revised magnitudes between Ms 7.0–7.4 [*Abe and Kanamori*, 1979; *Abe*, 1981; *Pacheco and Sykes*, 1992] and occur along the entire length of the Mariana forearc (Figure 2 and Table 1, events 6–13). Although some of these events are classified as intermediate depth earthquakes, and a few are located in the outer rise of the Pacific slab, they are included in the record due to the possibility of poor event locations in the early 1900s – up to 1° laterally and 30 km in depth for the best-located events, with earthquakes at 40–100 km depth being particularly problematic [*Gutenberg and Richter*, 1954]. In addition to uncertainty in earthquake locations and depths, magnitude estimates for these events have been calculated and revised numerous times [*Gutenberg and Richter*, 1954; *Gutenberg*, 1956; *Richter*, 1958; *Abe and Kanamori*, 1979; *Abe*, 1981; *Abe and Noguchi*, 1983; *Pacheco and Sykes*, 1992]; the most recent magnitude revisions are listed in Table 1.

[12] During 1825–1892, four large earthquakes and tsunamis are known to have affected the island of Guam. Estimates for the intensity of shaking on the island of Guam as compiled by *Maso* [1910] are included for all earthquakes occurring in 1825–1902 (Figure 2 and Table 1, events 1–5), but earthquake location, depth, and slip are unknown for the earliest events. Large, shallow thrust earthquakes often create tsunamis; however large extensional earthquakes in the bending Pacific plate at the Mariana trench have also produced tsunamis [*Satake et al.*, 1992; *Yoshida et al.*, 1992]. Therefore although significant damage and records of tsunamis on Guam exist, these tsunamis may not have been generated by shallow thrust earthquakes.

[13] The seismic record used by *Pacheco et al.* [1993] to compute seismic coupling coefficients along this margin included only two large events: 1902 Ms 7.4 occurring near 18°N, 146°E and 1934 Ms 7.1 occurring near 22.5°N, 144°E (Figure 2 and Table 1, events 5 and 10). No shallow thrust earthquakes larger than Ms 7.4 have been recorded and clearly located in the central and northern parts of the Mariana Islands during 1897 to 2010 [*Gutenberg and Richter*, 1954; *Abe and Kanamori*, 1979; *Abe*,

Figure 1. Array geometry for the 2003–2004 Mariana Subduction Factory Imaging Experiment. (top) Complete array of stations along with bathymetry. (bottom left) Stations that returned good data for the period before August 2003, prior to failure of the MPL4n OBS. (bottom right) Station geometry following August 2003. Stations are indicated in both plots by colored triangles (dark blue: Guralp 40T; cyan: STS2; red: Japanese PMD OBS; dark gray: MPL4o OBS; and light gray: MPL4n OBS). Pacific plate convergence beneath the Mariana Forearc is shown by thick black arrows; rate of convergence as determined by *Kato et al.* [2003] is noted above each arrow. Thick red lines show the location of the back-arc spreading center. Inset map in Figure 1 (top) shows all subduction trenches (blue lines), spreading centers (red lines) and transform boundaries (green lines) in the vicinity of the Mariana subduction zone and the Philippine Sea.

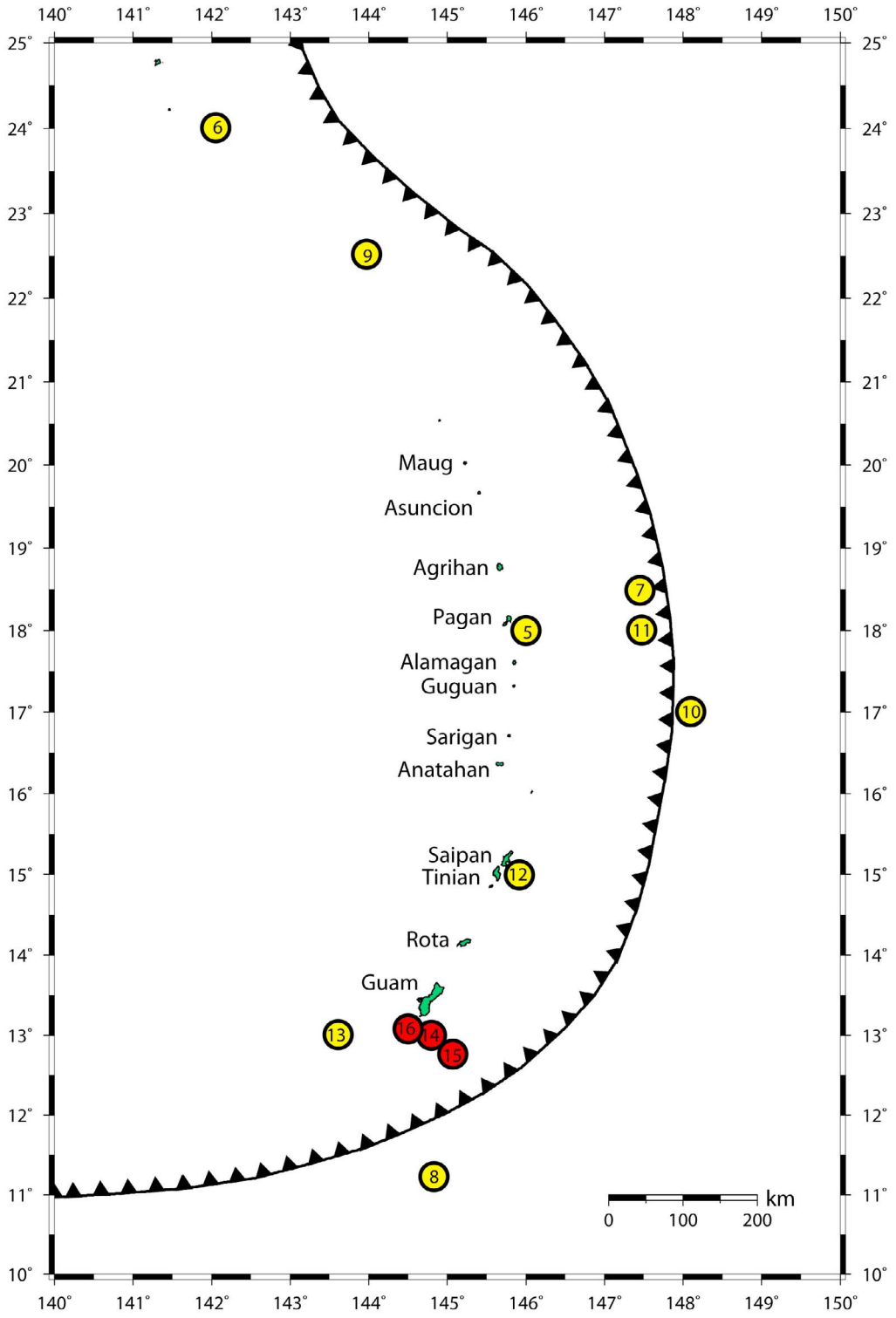

Figure 2. Locations for Events 5–16 listed in Table 1. All events are Mw or Ms ≥ 7.0, with depths less than 100 km, and are in or nearby the Mariana forearc. Epicenters of earthquakes occurring in 1902–1950 are indicated by yellow circles. Numbers within the yellow circles correspond to event numbers 5–13 listed in Table 1. Epicenters of thrust earthquakes occurring in 1951–2011 are indicated by red circles, and numbers within the red circles correspond to event numbers 14–16 in Table 1.

Table 2. Parameters Affecting Seismic Slip Coefficient and Maximum Earthquake Magnitude[a]

	Margin Length, L (km)	Seismogenic Width, W (km)	Time, T (yrs)	Convergence Rate, $\dot{u}_p$ (mm/yr)	Cumulative Moment, $\sum_i^N M_o^i$ (N-m)	Seismic Slip Coefficient, α	Moment Deficit (N-m)	Magnitude Deficit
1	1280	74	90	30	2.36 E20	0.0018	1.28 E23	9.34
2	1280	74	110	30	1.20 E21	0.0077	1.55 E23	9.39
3	1280	100	110	50	1.20 E21	0.0034	3.51 E23	9.63
4	560	100	110	40	4.62 E20	0.0037	1.23 E23	9.33

[a]Relationship used by *Pacheco et al.* [1993] for seismic slip coefficient: $\alpha = \frac{\dot{u}_s}{\dot{u}_p}$ where $\dot{u}_p$ is plate convergence rate and rate of seismic slip: $\dot{u}_s = \sum_i^N \frac{M_o^i}{\mu TWL}$. For all calculations, rigidity (μ) is 5.0E10 $\frac{N}{m^2}$. Parameters and results in the first row are those calculated by *Pacheco et al.* [1993] for the entire 1280 km length of the Mariana subduction zone. The second row incorporates a longer record and all shallow (depth < 100 km), M ≥ 7.0 seismicity nearby the Mariana forearc. The third row assumes a 100 km seismogenic width and recent (averaged along the margin) plate convergence rate from *Kato et al.* [2003]. The fourth row assumes the margin between 15 and 20°N and moment from all events in Table 1 at those latitudes. All calculations require that moment equivalent to a magnitude 9+ earthquake be released in order to compensate for the 110 years of Pacific plate convergence.

1981; *Pacheco and Sykes*, 1992]. Given the relationship for seismic coupling and fault parameters used by *Pacheco et al.* [1993], the absence of earthquakes larger than Ms 7.4 over the last ~110 years requires that a giant earthquake the size of the great Chilean or Alaskan earthquakes (Mw > 9) occur in order to seismically release the accumulated strain (Table 2, first row). Even assuming that every earthquake listed in Table 1 is a shallow thrust earthquake, the resulting seismic coupling coefficient is 0.0076 and requires that a Mw 9.39 earthquake occur every ~110 years in order to seismically release all accumulated strain (Table 2, second row). Although it is difficult to preclude this, most previous studies assume that the absence of earthquakes results from aseismic slip rather than an impending great megathrust earthquake [e.g., *Uyeda and Kanamori*, 1979].

2.3. The Marianas Seismogenic Zone and Aseismic Slip

[14] The two proposed explanations for Mariana aseismicity represent inherently different physical processes: reduction of normal force between the plates [*Scholz and Campos*, 1995] or reduced frictional strength between the plates due to rheological or fault zone properties [*Hyndman et al.*, 1997; *Peacock and Hyndman*, 1999; *Hyndman*, 2007]. In this section we review what is known about the Mariana shallow thrust zone in the context of the proposed explanations for the absence of great earthquakes.

2.3.1. Updip Limit of Seismogenic Zone

[15] Very little is known about the location of the updip limit in the Mariana seismogenic zone – previous studies of coupling have assumed a 10 km updip limit depth for all subduction zones [*Pacheco et al.*, 1993]. The onset of seismogenesis in continental subduction zones is classically perceived to begin near the base of the accretionary wedge, due to the compaction and cementation of sediments or presence of stronger crustal materials [*Byrne et al.*, 1988; *Marone and Scholz*, 1988; *Byrne and Fisher*, 1990; *Moore and Saffer*, 2001]. However, the Mariana island arc lacks an accretionary wedge. Hypotheses that the updip limit could be controlled by the phase transition of weak smectite clays to stronger illite clays [*Vrolijk*, 1990; *Moore and Saffer*, 2001] were found to not strongly affect onset of seismogenesis [*Saffer and Marone*, 2003]. More recently, the updip limit is thought to be controlled by decreasing pore pressure and fluid flux with depth as fluid producing diagenetic changes, such as the opal to quartz, smectite to illite, or hydrocarbon maturation cease [*Oleskevich et al.*, 1999; *Moore and Saffer*, 2001; *Spinelli and Saffer*, 2004]. Other diagenetic and low-grade metamorphic processes, such as pressure solution with subsequent quartz cementation, and zeolite-facies metamorphism with resulting cementation, are thought to strengthen the downgoing slab sediments [*Moore and Saffer*, 2001].

[16] Regardless of the underlying physical cause for the updip limit, there appears to be a correlation between the 100–150°C isotherm and the onset of thrust seismicity in subduction zones [*Hyndman and Wang*, 1993; *Oleskevich et al.*, 1999], although it is unclear whether the transition results directly from temperature or from other factors [*Saffer and Marone*, 2003]. In Costa Rica, a change in the age and temperature of the subducting seafloor correlates with a measurable offset in the location of the updip limit [*Harris and Wang*, 2002; *Newman et al.*, 2002; *DeShon et al.*, 2006; *Schwartz and DeShon*, 2007]. In the Mariana Islands, recent geochemical

work by *Hulme et al.* [2010] estimates the temperature conditions beneath Big Blue Seamount to be greater than 200°C. Given this and our current understanding of the initiation of seismogenesis, the updip limit should occur east of Big Blue Seamount [*Hyndman and Wang*, 1993; *Oleskevich et al.*, 1999].

2.3.2. Downdip Limit of Seismogenic Zone

[17] The transition from unstable slip producing earthquakes to ductile deformation beyond the downdip limit of the seismogenic zone has traditionally been interpreted as due to increasing temperature [*Hyndman and Wang*, 1993; *Tichelaar and Ruff*, 1993; *Hyndman et al.*, 1995; *Hyndman et al.*, 1997; *Harris and Wang*, 2002]. In continental subduction settings, the downdip limit was suggested to correspond to the 350–400°C isotherm with a transitional region of stable slip extending to 450°C [*Hyndman et al.*, 1995]. The downdip limit in regions such as the Mariana Islands, where the overriding plate has a thin crust and the downgoing plate contacts the forearc mantle, is suggested to correspond to higher temperatures, near 550°C [*Tichelaar and Ruff*, 1993].

[18] An alternate explanation suggests that the downdip limit is the boundary between overriding crust and serpentinized mantle wedge below, explained by aseismic layered serpentinite, brucite, and talc minerals within the mantle wedge [*Hyndman et al.*, 1997; *Peacock and Hyndman*, 1999; *Harris and Wang*, 2002; *Seno*, 2005]. This supposition relies on laboratory experiments indicating that these materials show stable sliding behavior at seismogenic depths [*Reinen et al.*, 1991; *Moore et al.*, 1997; *Hilairet et al.*, 2007; *Moore and Lockner*, 2007]. Earthquake producing slip depends on which serpentinite polymorph is present at that depth; antigorite, brucite and talc were found in one study by *Moore and Lockner* [2007] to be velocity-strengthening, while lizardite and chrysotile were velocity-weakening at experimental temperatures. Thermal modeling suggests that lizardite may be the dominant phase at shallow depths in the Mariana mantle wedge [*Wada and Wang*, 2009].

2.3.3. Variability of the Plate Interface Seismogenic Zone

[19] Some studies indicate variability in the sizes and characteristics of rupture with depth along the seismogenic width of subduction zones [e.g., *Hyndman et al.*, 1997; *Bilek and Lay*, 2000]. The subduction zones of Kermadec, Solomon, and Kamchatka exhibit a bimodal depth distribution of shallow thrust earthquakes [*Pacheco et al.*, 1993; *Hyndman et al.*, 1997], which has been explained by serpentinization at the shallowest mantle depths [*Hyndman et al.*, 1997]. In this model, the subducting plate slides aseismically while in contact with the serpentinized part of the mantle wedge but transitions back to stick-slip behavior deeper in the mantle wedge, where serpentinites are no longer stable and where the plate contact is not yet in the ductile deformation regime. In the Mariana Islands, serpentinites were similarly used to explain the seemingly narrow seismogenic width, although no second, deep seismogenic zone was observed [*Hyndman et al.*, 1997]. Source time durations for select circum-Pacific subduction zones, not including the Mariana Islands, show a general trend of decreasing, normalized rupture time with increasing depth of plate interface earthquake [*Bilek and Lay*, 1999, 2000]. The results were interpreted to be indicative of an increase in rigidity due to compaction and de-watering of subducting sediments [*Bilek and Lay*, 1999, 2000].

[20] Along-strike variability in interplate coupling as indicated by spatial distribution of shallow earthquakes [*Hasegawa et al.*, 2007] and earthquake rupture characteristics [*Ammon et al.*, 2005] has been noted to some extent in almost all subduction zones. Some subduction zones clearly show different degrees of locking versus stable sliding along strike [*Freymueller et al.*, 2008]. In the Mariana Islands, GPS data from the outer forearc are not available, so observations of creep and measures of interseismic locking cannot be obtained. The southern region may be more strongly coupled than the northern region [*Scholz and Campos*, 1995]; however this conclusion depends on the interpretation of large, shallow earthquakes in the historical records [*Pacheco et al.*, 1993] as well as the controversial 1993 Guam earthquake [*Tanioka et al.*, 1995; *Harada and Ishibashi*, 2008]. Observations of small earthquakes during a 2001 ocean bottom seismograph experiment in the Mariana Islands reveal distinct clusters of earthquakes - indicating that the plate interface may be slipping regularly in some regions, but may be either locked or slipping aseismically in other regions along the length of the subduction zone [*Shiobara et al.*, 2010].

[21] Along-strike changes in shallow thrust seismicity have been explained due to effects of subducting oceanic seamounts or other bathymetric highs [*Tanioka et al.*, 1997; *Bilek et al.*, 2003; *DeShon et al.*, 2003; *Shinohara et al.*, 2005; *Bilek*,

2007]. To the north, the Magellan Seamount Cluster and Dutton Ridge within the East Mariana Basin intersect the Mariana and Bonin trenches and are composed of Cretaceous volcanic seamounts (~100–120 Ma) [*Smith et al.*, 1989]. Intersecting the Mariana and Yap trenches in the south are the seamounts and islands of the Caroline Island chain, which is made up of young (less than ~12 Ma) volcanic seamounts and islands and atolls [*Keating et al.*, 1984]. At the trench east of Big Blue Seamount (~18.5°N) and the trench southeast of Celestial Seamount (~16°N), small, unnamed, ocean-floor seamounts in the vicinity of the larger Hussong and delCano Guyots are actively subducting, resulting in shallow depth of trench and disruption of the overriding Philippine plate (Figure 1) [*Gardner*, 2010; *Oakley et al.*, 2008]. *Oakley et al.* [2008] characterize the Mariana trench as four distinct sections, with the northern region near Big Blue as one section having increased seamount subduction, shallower trench, and displaced overriding plate toe.

3. Data Analysis

3.1. Data Sets

[22] During the 2003–2004 Mariana Subduction Factory Imaging Experiment we deployed 20 broadband seismometers and 58 ocean-bottom seismometers (OBS) from May/June 2003 until April/May 2004 (Figure 1). The 20 land seismometers were either Streckheisen STS-2 or Guralp CMG-40T sensors paired with REFTEK 72A-08 data loggers, and were deployed along the arc from Guam to Agrihan. At least one Streckheisen STS-2 sensor was deployed on each of the islands. The Guralp CMG-40T were deployed in dense arrays on the more southerly islands of Guam, Tinian, and Saipan. The instrument on the island of Anatahan experienced intermittent power failures due to ash cover on solar panels from the 2003 volcanic eruption [*Pozgay et al.*, 2005]. The rest of the land stations operated throughout the year. Of the 58 OBSs placed on the ocean floor, 50 used Mark Products L4 sensors [*Webb et al.*, 2001], with 15 using an older, 16-bit data logger (MPL4o) and 35 using a newer, 24-bit data logger (MPL4n). Due to an error in the firmware of the data logger, the newer, 24-bit model stopped recording after 50 days. The remaining 8 OBS used a Precision Measuring Devices sensor (PMD-WB2023LP) and were operated by University of Tokyo [*Shiobara et al.*, 2010]. The majority of the OBSs spanned from Pagan west into the backarc, with fourteen of the 58 OBSs deployed in the forearc (Figure 1). Station coordinates and dates of deployment are listed by *Pozgay et al.* [2007].

[23] In addition to data from the temporary Mariana deployment, we used phase arrival-time data from the International Seismological Centre (ISC bulletin, Thatcham, U. K., http://www.isc.ac.uk/search/index.html, 2010) for all Mariana forearc earthquakes located between 17.5 and 18.5°N during 1976–2008 for use in relative relocations. Depths and moment tensors of earthquakes from 1976 to 2008 in the same region were taken from the Global Centroid Moment Tensor (GCMT) database [*Dziewonski et al.*, 1981; www.globalcmt.org].

3.2. Earthquake Location

[24] As a first step, we used the Antelope software package to automatically detect and associate arrival times (www.brtt.com). The P and S wave arrival times were then manually picked and the earthquakes were located using the GENeric LOCation algorithm [*Pavlis et al.*, 2004]. Following this initial location, a relative location program, the hypocentroidal decomposition method of *Jordan and Sverdrup* [1981], was used to obtain better relative locations for all earthquakes with 15 or more P and S arrivals. In addition to the original method outlined by *Jordan and Sverdrup* [1981], we included the ability to calculate travel times according to a local velocity model for nearby stations. Our local P wave velocity model was obtained from the seismic refraction study of *Takahashi et al.* [2007], with S-wave velocities calculated from the P wave velocities using Vp/Vs of 1.8. This ratio is the global average Vp/Vs in the uppermost mantle [*Dziewonski and Anderson*, 1981] and was found by *Rossi et al.* [2006] at shallow mantle wedge depths (<80 km) in the Alaskan subduction zone.

[25] We also determined the relative positions of larger 1976–2008 teleseismic earthquakes using the hypocentroidal decomposition method and arrival times obtained from the ISC. We used P and PKP phase arrival data from all stations in the ISC Bulletin and S phase arrivals from stations closer than $\Delta = 20°$ to relocate all earthquakes in our study area for which a GCMT solution exists. The IASP91 velocity model was used to calculate teleseismic travel times [*Kennett and Engdahl*, 1991].

[26] Subduction zone earthquakes located with only teleseismic data often show a significant hypocenter bias due to the velocity structure of the downgoing slab [e.g., *Fujita et al.*, 1981], and teleseismic

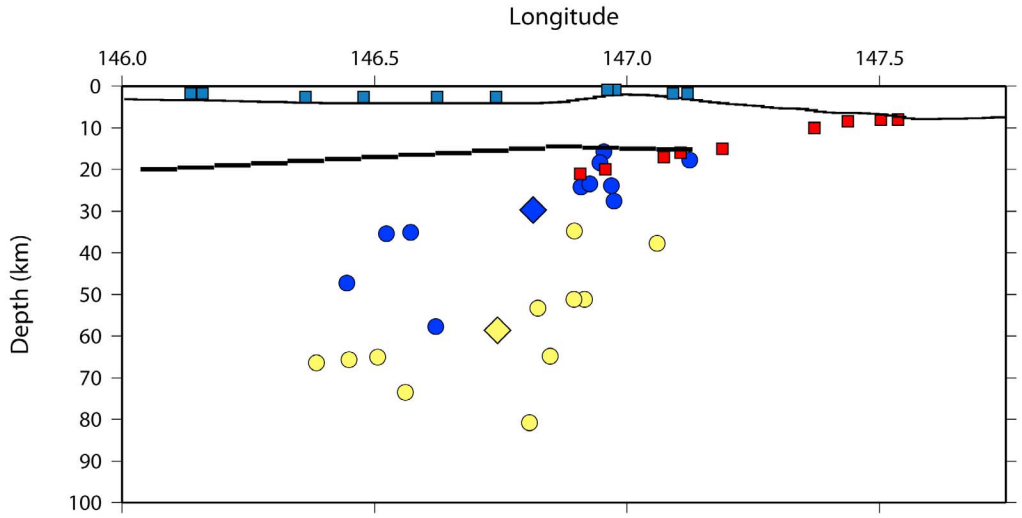

Figure 3. Image shows the shift between GCMT earthquakes relocated only with other teleseismic events (yellow circles; average location yellow diamond) and GCMT earthquakes relocated along with local Mariana events (blue circles; average location blue diamond). Red squares show the trace of the plate interface just south of the Big Blue Seamount as determined by *Oakley et al.* [2008]. Light blue squares show the location of forearc ocean-bottom seismometers during the 2003–2004 Mariana Subduction Factory Experiment. Black line shows the bathymetry of the forearc at 18°N. Thick black line shows the trace of the Moho in the region south of Celestrial Seamount, ~17°N, as determined by *Takahashi et al.* [2007].

location accuracy is particularly poor in the Mariana arc due to the nearly complete absence of stations to the east. Teleseismic earthquakes recorded during 2003–2004 that were also recorded by the local array allow us to test and correct the teleseismic locations for bias due to unmodeled, large scale velocity structure of the earth. Comparison of the hypocenters for 2003–2004 earthquakes computed using only teleseismic arrivals with the hypocenters computed using only local array data reveal a significant discrepancy between teleseismic and local array locations; those with local arrival data show a shift to shallower depths than those with only teleseismic arrivals. The uncertainty ellipsoids of the events computed with local arrivals are much smaller than uncertainties for the teleseismic data sets. We conclude that the locally recorded earthquakes have inherently better location and depth resolution due to the presence of the array almost directly above the source region as well as the use of a local velocity model. Furthermore, the shallow locally recorded earthquakes align with the deepest part of the plate interface determined from seismic reflection data [*Oakley et al.*, 2008].

[27] In order to better constrain the absolute locations of the globally recorded earthquakes, we simultaneously located them along with the locally recorded earthquakes using the hypocentroidal decomposition method. The fact that larger earthquakes from 2003 to 2004 were recorded by both local and teleseismic station sets allowed the local data to provide constraints on the absolute position of all the earthquakes and resulted in reduced uncertainty for teleseismically recorded events (Figure 3).

3.3. Focal Mechanism Determination

[28] We determined focal mechanisms for events in 2003–2004 using a grid-search waveform inversion method based on reflectivity synthetic seismograms [*Kennett*, 1983]. Synthetics were calculated for three fundamental double-couple source geometries [*Langston and Helmberger*, 1975], and then linearly combined to obtain synthetics for each focal mechanism in the grid search. Vertical and transverse component records from the land Streckeisen STS-2 seismographs as well as the vertical components from Lamont-Doherty ocean-bottom seismometers were used in the inversion. The horizontal components from the ocean-bottom seismometers were not used due to the high level of long-period noise as well as some uncertainty in the orientations of the instruments. While the addition of the OBSs helped to increase the number of available signals for inversion, generally the low frequencies from the OBSs were noisier than those recorded on land due

to their location on the seafloor. Furthermore, the 16-bit OBSs closest to the study region were sometimes omitted due to signal clipping.

[29] For each station at which a clear and complete signal was recorded, the trace was filtered from 0.03 to 0.08 Hz and matched with synthetics computed for the same frequencies and the full range of possible fault solutions. We further refined event depths by varying our inversions over depths of +/−20 km from the initial value. The solution misfit was defined as the squared difference between the observed and synthetic waveforms, and a cross correlation method was used to allow the synthetic times to vary by up to 2–3 s to minimize the effect of small changes in velocity structure. After finding the region of the parameter space for which the synthetics fit best, the grid search was narrowed in scope in order to further refine the solution. The results from the inversion were typically not reliable for earthquakes smaller than Ml 4.2, due to poor signal-to-noise ratios. Of the 188 earthquakes that we located in the shallow Big Blue region, only 4 of these were large enough to have clean low-frequency signal.

[30] We tested our method on the only shallow earthquake to occur near the study region during the time of our deployment that was large enough to have a GCMT solution (Figure 4). The GCMT solution for this indicates a shallowly dipping, slightly oblique thrust faulting mechanism, but has a poorly constrained depth that was fixed at 15 km in the GCMT inversion. The GCMT solution contains a small CLVD component, but is predominantly double-couple with a strike of 7°, dip of 75°, and slip of 120° for the first fault plane and a strike of 124°, dip of 31°, and slip of 31° for the other fault plane of the mechanism. We assume that the north-south striking nodal plane is the plane of rupture; this is consistent with the north-south strike of the subduction zone. Our relocation and waveform modeling of this event indicated that the earthquake depth was slightly deeper (20–25 km). Grid-search results indicated two different mechanisms for which the synthetics had a small misfit to the data; this is likely due to the limited azimuthal coverage of the array, as most of stations were located to the southwest of the earthquake cluster. For the GCMT earthquake one of our best fitting focal mechanisms was a slightly oblique N-S striking and west dipping shallow thrust mechanism (fault plane 1: strike 0°, dip 70°, slip 125°; fault plane 2: strike 115°, dip 40°, slip 32°), and the other well-fitting mechanism was an E-W striking oblique normal faulting event (fault plane 1: strike 91°, dip 43°, slip 349°; fault plane 2: strike 189°, dip 83°, slip 226°). Although synthetics from both types of focal mechanisms fit the waveform data well, the N-S striking thrust mechanism had a slightly smaller misfit to the data than the other mechanism and was similar to the GCMT solution. After verifying our waveform inversion solution with the GCMT earthquake, we applied the technique to four other forearc earthquakes with Ml 4.2–4.7 occurring during June 2003-April 2004.

[31] We also attempted to determine focal mechanism solutions for small, local earthquakes using first-motions of the P and S waves as well as SV/SH amplitude ratios inputted into the commonly used FOCMEC program [*Snoke et al.*, 1984]. Examination revealed that the first motions for earthquakes in our region, specifically SV and SH phases, were often ambiguous, and that the station geometry was poor for focal mechanism determination with first motion data. The limited number of clear constraints resulted in non-unique solutions, so the first motion results are not used in this paper.

4. Results

4.1. Earthquake Locations

[32] The yearlong experiment recorded 3,452 earthquakes throughout the entire region of the Mariana Islands. Of these detected earthquakes, just over 1000 were located in the shallow forearc (16–19°N, 145.5–148°E, 0–120 km) with 10 or more P and S arrivals (Figure 5). We observed prominent clusters of earthquakes in the region directly west of Big Blue seamount (17.5–19°N), with significantly fewer events in the forearc south of Big Blue (16–17.5°N) (Figure 5). The proximity of event locations to the densest region of the 2003–2004 seismic array suggests at first that detection capability is dependent on array geometry; however locations for larger, easily detectable, earthquakes recorded during this time reveal that the increased number of earthquakes near Big Blue Seamount is not dependent on array limitations (Figure 6). These larger earthquakes have Ml $\geq$ 3; the estimated magnitude of completeness for our array is Ml ~ 2–2.5. We also consider that the observed pattern of earthquakes may be temporally biased. Yet, the cluster of local events recorded during 2003–2004 coincides with noted patches of seismicity from an OBS deployment in 2001 [*Shiobara et al.*, 2010].

[33] We calculated relative relocations for 188 shallow, locally recorded earthquakes with 15+ arrivals

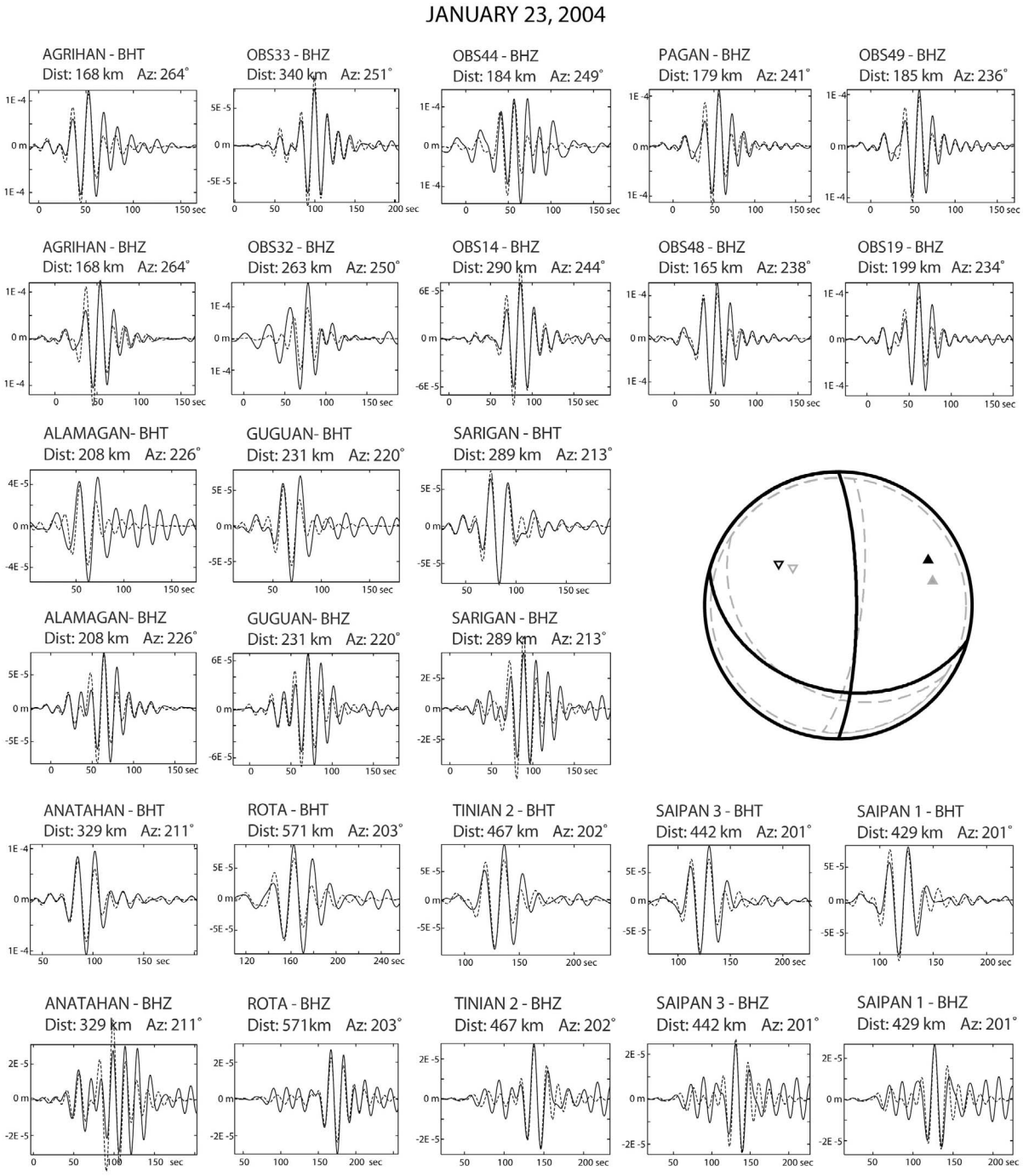

Figure 4. Example of data (solid line) and synthetics (dashed line) from the stations used in our waveform inversion for the 23 January 2004 event, for which a GCMT solution has been determined. Station azimuths range from 260° in the north on Agrihan island to 201° in the south at Rota island. The solid black lines of the focal mechanism show the fault planes from this study (P axis: solid black triangle; T axis: black outlined, inverted triangle), while the dashed gray lines show the best fitting double couple from the GCMT solution (P axis: solid gray triangle; T axis: gray outlined, inverted triangle).

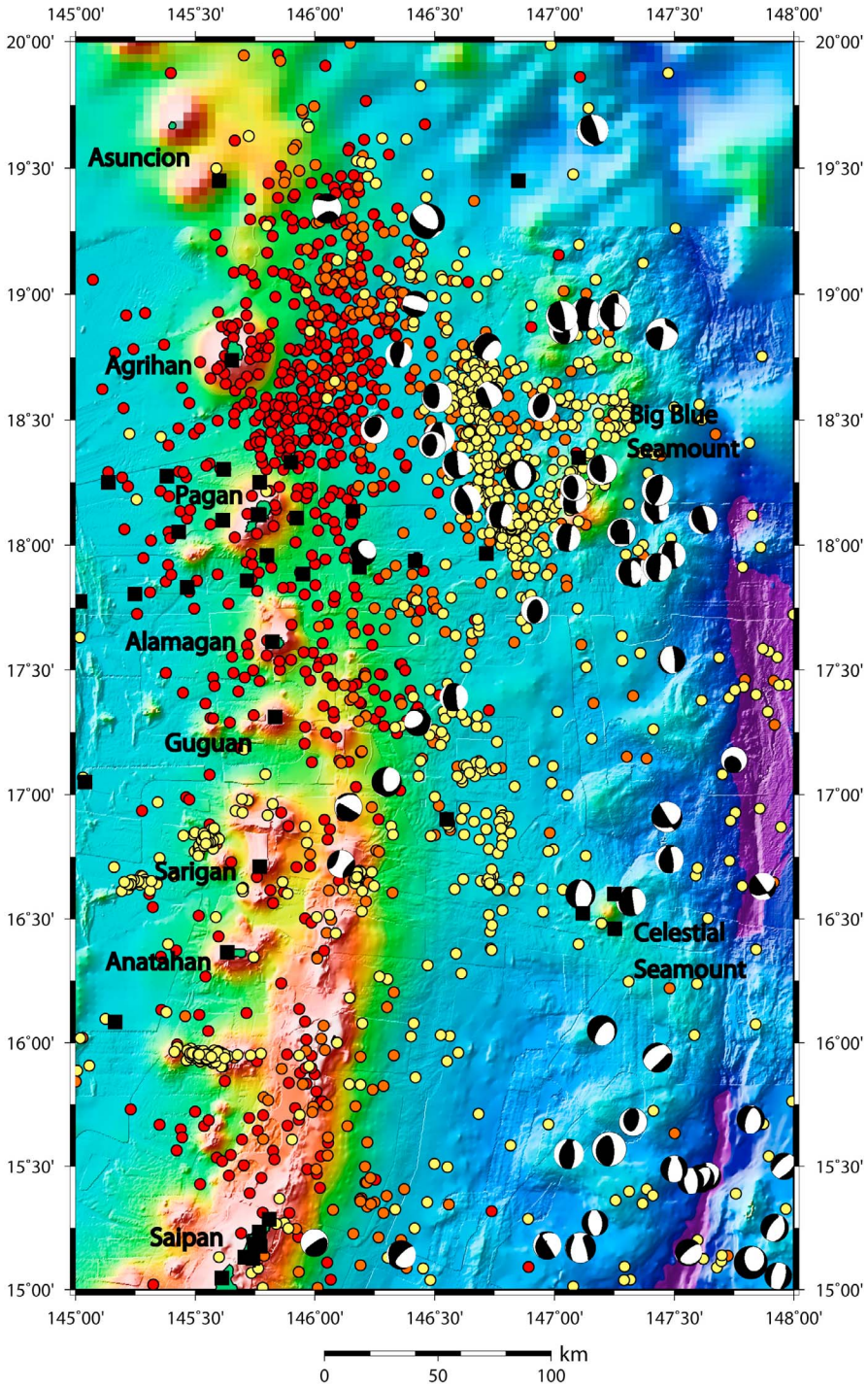

Figure 5. Locations of earthquakes in the Mariana subduction zone from 15 to 20°N prior to relocation. Yellow circles indicate earthquakes at 0–50 km depth; orange circles are earthquakes at 50–100 km depth; red circles are earthquakes deeper than 100 km. Black squares show the locations of land and ocean-bottom seismographs. GCMT solutions from 1976 to 2008 are plotted on a lower-hemisphere projection and colored black (compressive quadrants) and white (extensional quadrants).

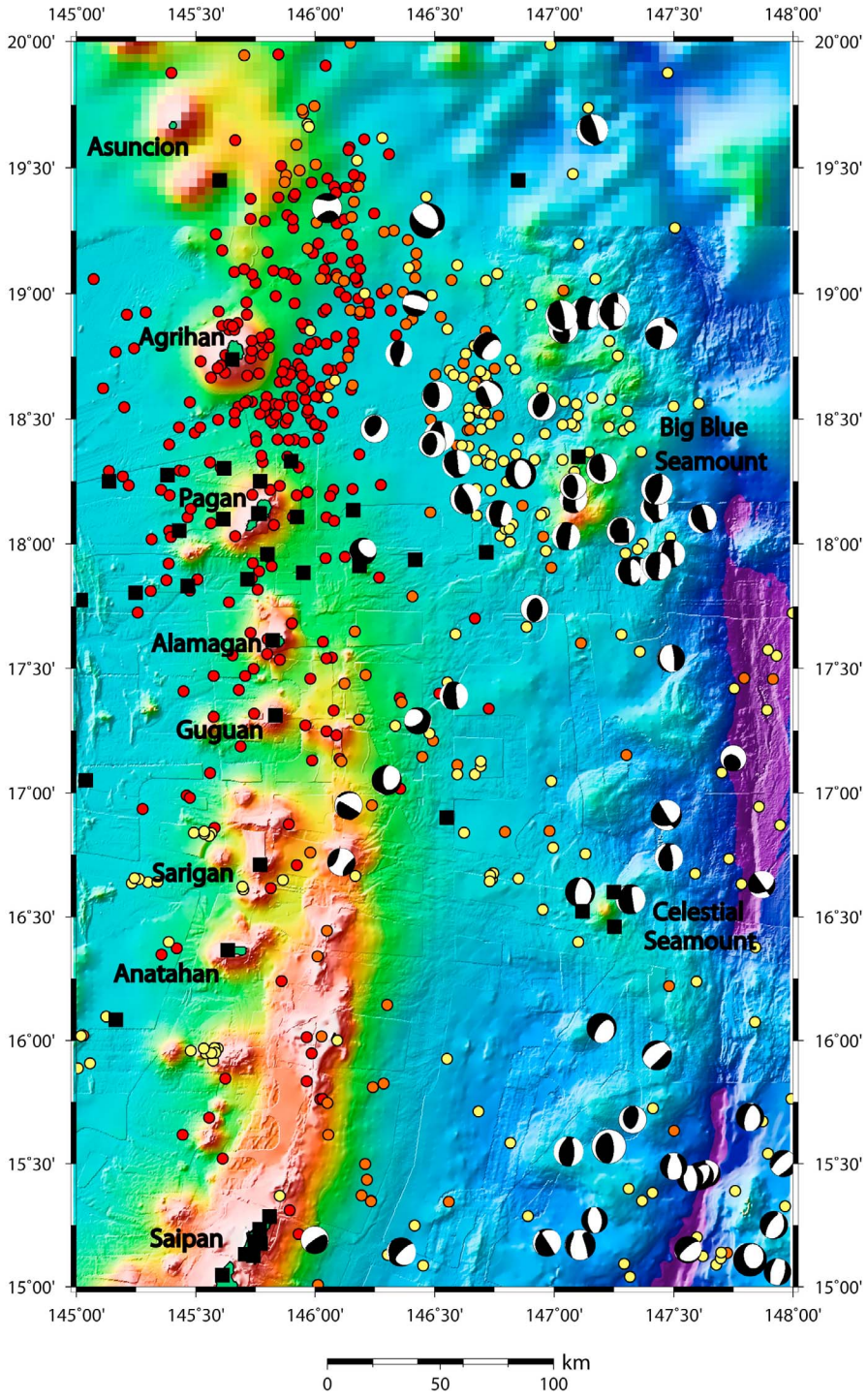

Figure 6. Locations of earthquakes, with magnitude greater than or equal to Ml 3.0, in the Mariana subduction zone from 15 to 20°N prior to relocation. Yellow circles indicate earthquakes at 0–50 km depth; orange circles are earthquakes at 50–100 km depth; red circles are earthquakes deeper than 100 km. Black squares show the locations of land and ocean-bottom seismographs. GCMT solutions are plotted on a lower-hemisphere projection and colored black (compressive quadrants) and white (extensional quadrants).

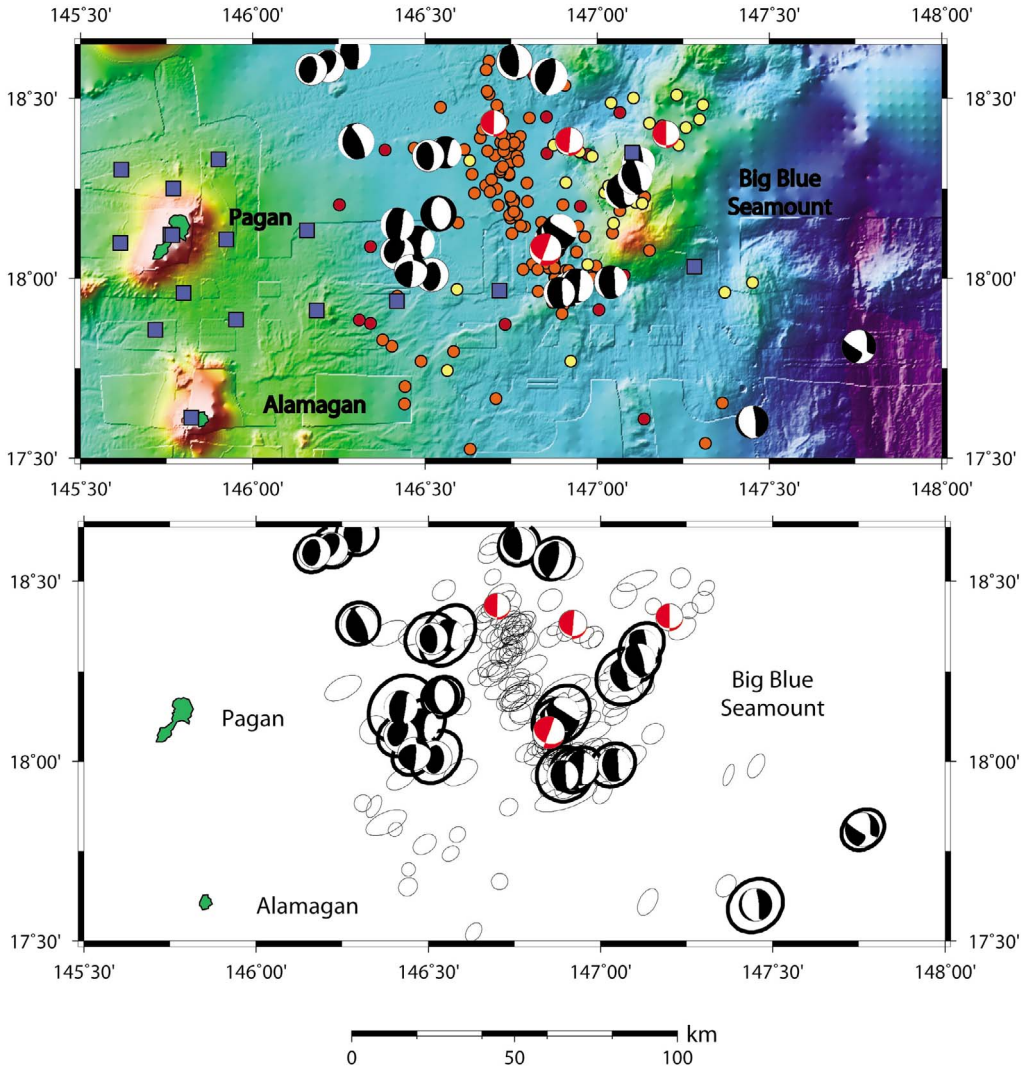

Figure 7. (top) Map view of study region showing locally recorded seismicity during 2003–2004 in the vicinity of Big Blue Seamount. Yellow circles indicate earthquakes occurring at 0–30 km depth. Orange circles indicate earthquakes occurring at 30–60 km depth. Dark red circles indicate earthquakes occurring at 60–100 km depth. Relocated GCMT earthquakes occurring between 17.5 and 18.5°N during 1976–2008 with double-couple focal mechanisms plotted on a lower-hemisphere projection are colored black (compressive quadrants) and white (extensional quadrants). Focal mechanisms determined in this study for the largest local earthquakes occurring during 2003–2004 are colored red (compressive quadrants) and white (extensional quadrants). (bottom) Map view of study region, omitting bathymetry, showing the 2σ confidence ellipsoids projected onto the latitude-longitude plane. Ellipses with a thin, black outline show the confidence in horizontal location for locally recorded earthquakes during 2003–2004. Ellipses with a thick, black outline show the confidence in horizontal location for GCMT earthquakes from 1976 to 2008. Focal mechanisms are shown for GCMT solutions and 2003–2004 earthquakes as described above.

within the vicinity of OBSs in the Big Blue Seamount region (17.5–18.5°N, 146–148°E, 0–80 km) (Figures 7 and 8). These earthquakes have local magnitudes ranging from Ml 1.6 to 4.7. Of the 158 earthquakes recorded by the ISC during 1976–2008 in the Big Blue Seamount region, we relocated the 25 that have a GCMT solution. Twenty-two of these are thrust type earthquakes.

[34] The locations and depths of the local and GCMT earthquakes cluster along a plane representing the Mariana shallow thrust zone extending from 20 km down to 60 km (Figure 8). This plane of seismicity shows continuance of the plate interface as determined by multichannel seismic reflection along a survey line just south of Big Blue Seamount [*Oakley et al.*, 2008]. The cluster of small

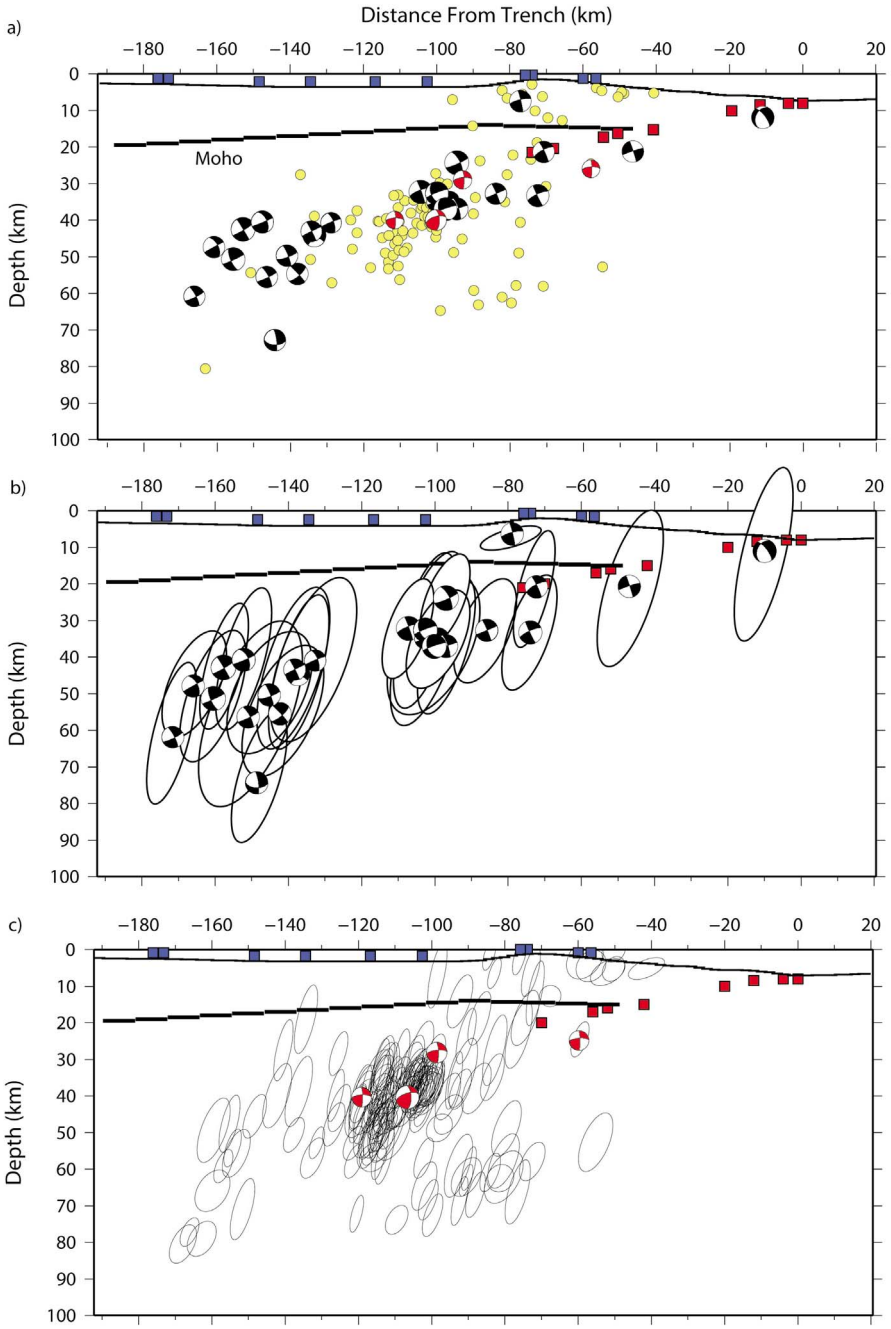

Figure 8. (a) Cross-section of all 1976–2008 relocated GCMT earthquakes along with 2003–2004 locally recorded earthquakes. Double-couple focal mechanisms for GCMT earthquakes (black) and this study (red) are shown in side-projection. Yellow circles show the locations of our locally recorded earthquakes. Red squares show the trace of the plate interface just south of the Big Blue Seamount as determined by *Oakley et al.* [2008]. Light blue squares show the location of forearc ocean-bottom seismometers during the 2003–2004 Mariana Subduction Factory Experiment. Black line shows the bathymetry of the forearc at 18°N. Thick black line shows the trace of the Moho in the region south of Celestrial Seamount, ~17°N, as determined by *Takahashi et al.* [2007]. (b) Cross-sectional view showing the 2σ confidence ellipsoids for GCMT earthquakes projected onto the vertical plane. Large ellipses with a thick, black outline show the confidence in location and depth for GCMT earthquakes from 1976 to 2008. Focal mechanisms are shown for GCMT solutions as described above. (c) Cross-sectional view showing the 2σ confidence ellipsoids for locally recorded earthquakes projected onto the vertical plane. Small ellipses with a thin, black outline show the confidence in location and depth for locally recorded earthquakes during 2003–2004. Focal mechanisms shown in side-projection determined for 2003–2004 earthquakes in this study are shown in red.

Table 3. Waveform Inversion Results: Earthquake Locations and Fault Orientations

Date	Time (UTC)	Latitude (°N)	Longitude (°E)	Depth (km)	Strike (deg)	Dip (deg)	Slip (deg)	Mw
7 Jul 2003	17:29:41	18.37	147.23	26	0	89	110	4.3
8 Jul 2003	09:12:38	18.43	146.70	40	91	21	0	4.2
15 Jul 2003	14:51:32	18.08	146.85	40	20	89	123	5.1
23 Jan 2004	03:39:14	18.91	147.24	22.5	0	79	125	5.6
17 Apr 2004	21:56:30	18.38	146.92	29	5	89	112	4.5

earthquakes occurring immediately west of the Big Blue Seamount, elongated in a direction slightly west of north, is clearly delineated in the relative relocation results (Figure 7). Most of these shallow earthquakes occur 100–120 km west of the trench and have depths of 30–45 km (Figure 8). 95% uncertainties in the vertical direction are generally less than ~5–10 km and lateral uncertainties are generally less than 5 km. A few earthquakes have depths well beneath the thrust interface, and are likely related to the updip limit of the Mariana double seismic zone [*Barklage*, 2010; *Shiobara et al.*, 2010]. During the local deployment, no earthquakes shallower than 30 km occurred directly beneath the summit of the Big Blue serpentinite mud volcano, located just trench-ward of the majority of our recorded seismicity. The shallowest GCMT thrust earthquakes occur just west of Big Blue Seamount or in the forearc north of Big Blue. The deeper GCMT thrust earthquakes are located ~30 km west of the shallow section of GCMT thrust earthquakes, with a noticeable gap separating the two groups.

4.2. Focal Mechanisms

[35] All of the earthquakes for which we inverted waveforms to obtain the source had two best fitting focal mechanisms: a N-S striking thrust mechanism and an E-W striking oblique normal mechanism. As was discussed in the previous section for the GCMT event, this non-uniqueness occurs because the predicted waveforms are similar for the two mechanism types within the limited azimuthal range of our recording stations. Because the thrust focal mechanism fit the well-recorded GCMT event better, despite having two separate mechanisms with low misfit to the data, and because none of the GCMT earthquakes found in the region surrounding the Big Blue seamount show E-W striking oblique normal faulting, we select the N-S oriented thrust faulting mechanisms from our waveform inversions as the preferred sense of rupture (Figure 7 and Table 3). This assumption, based on tectonic considerations is strengthened by the fact that many of the smaller magnitude earthquakes without focal mechanisms occur in the region immediately surrounding these thrust earthquakes; we presume that these also represent thrust faulting on a shallowly westward dipping plane (Figure 8). The earthquakes occur along the top of the slab, and define the apparent location of the Mariana shallow megathrust fault.

5. Discussion

5.1. Depth Extent of the Interplate Seismogenic Zone

[36] The seismogenic zone of the Northern Mariana plate interface, as defined by shallowly dipping thrust earthquakes, initiates about 60 km west of the trench at a depth of 20 km and ceases 160 km west of the trench at 60 km depth (Figure 8). This gives an average dip of 21° degrees and a seismogenic zone width of about 100 km. This is significantly larger than the width argued by *Hyndman et al.* [1997] and larger than the 74 km previously estimated by *Pacheco et al.* [1993]. Other island arc regions determined by *Pacheco et al.* [1993] have seismogenic widths ranging from 53 km in the Rat Islands and South Sandwich Islands up to 113 km in the Eastern Aleutians, making the Northern Mariana plate interface toward the wider end of this range.

[37] The updip limit of thrust seismicity occurs approximately beneath Big Blue Seamount at the deepest part of the plate interface imaged in the seismic reflection study of *Oakley et al.* [2008]. The onset of seismicity also corresponds to the proposed 200°C isotherm beneath Big Blue Seamount [*Hulme et al.*, 2010] and the intersection between subducting slab and the forearc Moho [*Takahashi et al.*, 2007]. Plate interface thrust earthquakes continue for 40 km deeper than the Moho. Thus nearly all observed Mariana thrust zone seismicity occurs at the interface between the forearc mantle and the downgoing crust. Along with the observed 100 km width of the seismogenic zone, this contradicts the view that the aseismicity for large events along the Mariana subduction zone is a result of an anomalously narrow seismogenic

width [*Hyndman et al.*, 1997; *Peacock and Hyndman*, 1999; *Hyndman*, 2007]. In northeast Japan, a setting with similarly old Pacific oceanic crust, shallow thrust seismicity continues well below the Moho [*Igarashi et al.*, 2001; *Shinohara et al.*, 2005]. If downdip limit corresponds to temperature, then the 550°C isotherm as determined by *Tichelaar and Ruff* [1993] for oceanic settings may be expected at depth of ~60 km and distance of ~160 km from the trench in Northern Mariana. We conclude that plate interface earthquakes are not limited by the shallow depth of the crust-mantle boundary in the Northern Mariana subduction zone.

[38] Our observations of updip and downdip limits may not fully identify the absolute boundaries of the seismogenic thrust, but rather identify a lower end estimate of seismogenic width. Geodetic results from Costa Rica show that the shallowest portion of the seismogenic zone is locked [*Norabuena et al.*, 2004] and do not match with updip limit estimates from microseismicity [*DeShon et al.*, 2006; *Schwartz and DeShon*, 2007]. If the Mariana plate interface is comparable to Costa Rica in this respect, then the shallowest section of the plate interface may be locked rather than sliding stably. Locking along this crust-crust contact would serve to increase the width of the seismogenic zone, which would further increase estimates of seismic slip deficits in this region. Furthermore, rupture along the shallow portion of the plate interface would increase the possibility of hazards associated with tsunamis. From recorded local seismicity, we cannot conclude whether this part of the contact is locked or sliding aseismically; rather we conclude only that underthrusting earthquakes were observed to begin at ~20 km depth.

[39] Estimates of seismic coupling from Table 2 show that despite the addition of other $M \geq 7.0$ earthquakes, the percentage of slip occurring seismically is still very small. Our estimate of a larger seismogenic plate interface affects calculation of seismic coupling even more. The third row of Table 2 illustrates that with more recent estimates of plate convergence rates [*Kato et al.*, 2003] and seismogenic width, the percentage of seismic slip decreases even further, causing the deficit in seismic moment to become unrealistically large (greater than the 1960 Chilean earthquake). Even if we consider only the Northern Mariana seismogenic zone, spanning from 15 to 19°N, and the events occurring within that region (Table 2, fourth row), the deficit in seismic slip requires that an earthquake greater than Mw 9 occur to compensate for the lack of large earthquakes. These simple calculations argue that because Mw > 9 earthquakes do not occur in this region every ~100 years as necessary to compensate for plate convergence rates, a significant amount of plate convergence must be accommodated through some mechanism allowing aseismic slip between plates.

5.2. Change in Seismogenesis With Depth

[40] Seismogenic behavior continues along the entire depth range of the shallow plate interface in the Northern Mariana subduction zone but shows changes with depth. Larger magnitude earthquakes, represented by the 1976–2008 GCMT solutions with Mw 4.9–5.8 are located both updip and downdip of the cluster of small, locally recorded earthquakes. The GCMT events occur mostly within a shallow region 70–100 km west of the trench and in a deeper region of the subduction zone 130–160 km west of the trench, with a prominent gap between them (Figure 8). If we consider only earthquakes that occur within +/−10 km in the vertical direction of our inferred seismogenic zone and observe how many locally recorded and GCMT earthquakes (as a percentage of the total number) occur at increasing distances from the trench, we note that many small, locally recorded earthquakes occur within the observed gap in GCMT earthquakes (Figure 9). Although our array recorded local events only during 2003–2004, *Shiobara et al.* [2010] recorded similar clusters of earthquakes during 2001. Therefore we infer that the clusters of small earthquakes are not a short-lived burst of seismicity, but rather a long-term feature.

[41] The pattern of seismicity occurring during 2003–2004 is reminiscent of patterns observed at the Nicoya Peninsula of Costa Rica, where the majority of recorded earthquakes occurred at intermediate depths along the seismogenic zone, both downdip and updip of stronger regions of partial locking as determined by geodesy [*Norabuena et al.*, 2004; *DeShon et al.*, 2006]. A study of varying frequency-magnitude distributions (b-values) along dip of the Costa Rica seismogenic zone indicated that shallow depths had lower b-values, presumably due to greater interplate locking as observed by geodesy [*Norabuena et al.*, 2004; *Ghosh et al.*, 2008]. As noted, our seismic results cannot determine whether the portion of the plate boundary updip from our observed seismicity is locked or slipping aseismically; however the frequency of small earthquakes at intermediate depths within the seismogenic zone indicates that the interface further updip from this

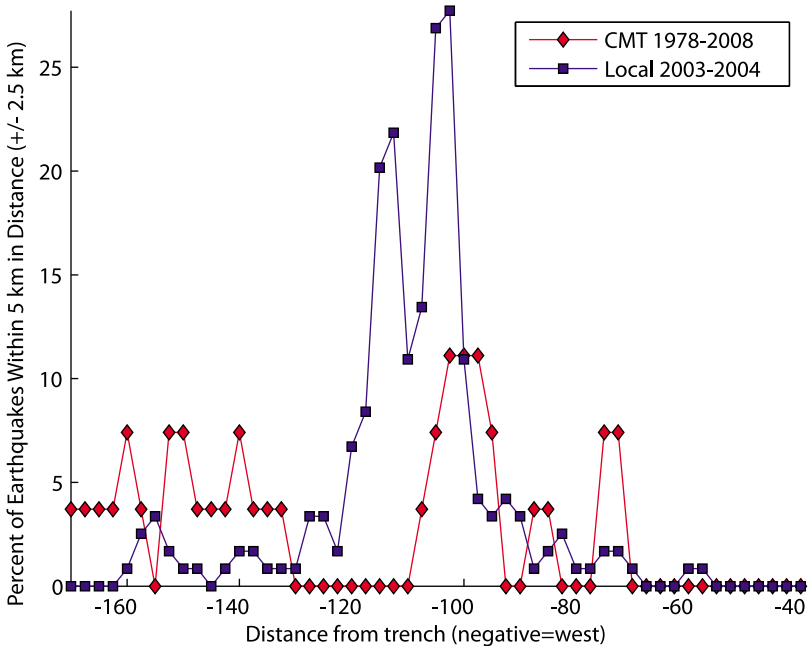

Figure 9. The occurrence of 2003–2004 locally recorded earthquakes (blue squares and blue line) and 1976–2008 GCMT thrust earthquakes (red squares and red line) within the seismogenic zone is plotted with increasing distance from the trench. Local and GCMT earthquakes are plotted as a percentage of the total amount of local and GCMT seismicity. All earthquakes shallower than 70 km and also within 10 km vertically of the observed seismogenic zone were culled from the entire region shown in Figure 8. For every 2.5 km of distance from the trench, the total number of earthquakes within a 5 km window (2.5 km to either side) was counted and represented as percentage of the total number of earthquakes of the same type (GCMT or local) occurring within the region inferred to be the seismogenic zone. Most of the locally recorded earthquakes occur in a region where few GCMT earthquakes are located, suggesting some mechanism inhibiting the occurrence of larger shallow thrust earthquakes in this middle region of the seismogenic zone.

may be more strongly coupled, and perhaps even locked at depths shallower than ~20 km.

[42] The pattern of GCMT seismicity is also similar to the Kermadec, Solomon, and Kamchatka subduction zones, which show a gap in the depth distribution of shallow GCMT thrust earthquakes [*Pacheco et al.*, 1993; *Hyndman et al.*, 1997]. As mentioned previously, *Hyndman et al.* [1997] hypothesized that gaps at shallow mantle depths along the plate interface in island arc subduction zones could be explained by aseismic mantle serpentinites, but suggested that the Mariana forearc was sufficiently serpentinized that the lower zone of unstable sliding was not reached, and that shallow thrust earthquakes were largely limited to the upper 20 km. Our results using more accurate relative locations of both locally and teleseismically recorded earthquakes contradict this view. The Northern Mariana plate interface seismogenic zone has a notable gap in GCMT events along the plate interface from 100 to 130 km west of the trench at depths of 30–45 km, which corresponds well with the location of the prominent cluster of smaller magnitude earthquakes. However, larger GCMT thrust faulting events clearly resume at deeper depths.

[43] We propose that the relationship of small and large earthquakes as shown by locally recorded and GCMT events in Figure 8 is due to a change in the magnitudes of earthquakes occurring with depth in the seismogenic zone (Figure 9) that may result from variations in the degree of serpentinization or the presence of high pore fluid pressures. A higher degree of serpentinization could cause most of the seismogenic zone between depths of 30–45 km to show an increased amount of stable sliding and small earthquakes relative to regions updip or downdip. In this case, only small patches of the fault contacting unserpentinized overriding mantle would exhibit stick-slip behavior, and the small size of these "asperities" would result in an absence of larger earthquakes and a predominance of smaller earthquakes within this region. Alternatively, the changing character of seismogenesis with depth could result from a greater abundance of fluids and higher pore pressures within the megathrust fault from 30 to 45 km. Expulsion of fluids from pore water and loosely bound structural water within

subducting igneous crust could be a potential source for additional fluids at these depths [*Jarrard*, 2003]. Increased pore pressures resulting from slab dehydration have been suggested to enable the occurrence of non-volcanic tremor and low frequency earthquakes in other subduction zones such as Cascadia and southwest Japan [*Shelly et al.*, 2006; *Audet et al.*, 2009]; similarly we expect this mechanism could prove to be a plausible explanation for increased occurrence of smaller magnitude earthquakes with depth. Non-volcanic tremor and low frequency earthquakes have not been detected at the Mariana subduction zone to date; attempts made to observe tremor using the 2003–2004 forearc OBS has been unsuccessful due to presence of other noise in the water column.

[44] Another possibility is that variations in seismic characteristics with depth result from changes in the roughness of the surface of the subducted slab [*Tanioka et al.*, 1997; *Yamanaka and Kikuchi*, 2004; *Bilek*, 2007]. Physical structures of varying sizes, whether subducted seamounts, horst and graben structures, or ridges, would increase normal stress in some regions while decrease normal stress in others – thus producing a variation in size and frequency of earthquakes along the interface. This same mechanism has been invoked to explain patches of increased seismicity in other subduction zones such as Northeast Japan [*Tanioka et al.*, 1997; *Yamanaka and Kikuchi*, 2004] and Costa Rica [*Bilek et al.*, 2003; *DeShon et al.*, 2003; *Ghosh et al.*, 2008]. Large seamounts on the seafloor east of the Mariana Trench implies that the recently subducted seafloor is similarly rough and makes plate interface roughness a distinct possibility for the location and frequent occurrence of GCMT earthquakes beneath different portions of the Northern Mariana forearc. However, this possibility is difficult to test because the positions of previously subducted bathymetric features cannot be determined with confidence.

5.3. Along-Strike Plate Interface Heterogeneity

[45] The distinct cluster of local earthquakes in the vicinity of Big Blue Seamount does not continue along the entire length of the Mariana subduction zone. Although sufficient seismic detection capabilities existed to the south, at latitudes of 16°–17.5°N, significantly fewer local earthquakes are found. This observation suggests significant lateral variability in plate interface and seismogenic characteristics.

[46] Serpentinization of overriding forearc mantle need not be homogenous along the entire length of the subduction zone; along-strike changes in amount of mantle serpentinization could be created by variations in shallow water flux from the slab. In North and Central Mariana forearcs, results from Rayleigh wave phase velocities indicate lower shear velocities in the central portion of the forearc mantle than in the Northern forearc mantle near Big Blue [*Pyle et al.*, 2010]. If this heterogeneity is due to mantle serpentinization, then some regions of the forearc may be more highly serpentinized than others [*Pyle et al.*, 2010]. Similarly, heterogeneity in mantle serpentinization was proposed in the Northeast Japan mantle forearc [*Yamamoto et al.*, 2008]; regions of low Vp/Vs typical of unaltered mantle wedge material were found to correlate well with increased occurrence of large Mw > 7.0 earthquakes in the off-Miyagi region and regions of high Vp/Vs typical of serpentinized mantle wedge were found to correlate well with lack of large Mw < 7.0 earthquakes off-Fukushima.

[47] Similar to serpentinization of forearc mantle, fluids present along the seismogenic plate interface can be heterogeneous along-strike. Expulsion of water from the subducting slab at shallow plate interface depths occurs due to dewatering of sediments and water trapped within the top of the crust [*Jarrard*, 2003; *Hacker*, 2008; *Oakley et al.*, 2008]. The Mariana subducting slab is generally lacking in sediment in comparison to other margins [*Oakley et al.*, 2008]. Yet recent multichannel seismic reflection data from *Oakley et al.* [2008] reveals that the sediment layer thickness increases from 1 km in Northern Mariana, near our study area, to 2 km in Central Mariana, south of our study area. Sediments on the Pacific plate are composed of thin layers of cherts and more water-rich clays, with regions of thickened volcaniclastic sediment near seafloor seamounts [*Hacker*, 2008; *Oakley et al.*, 2008]. The change in amount of subducted sediment could provide an increase in water available for expulsion at the shallowest depths in the forearc south of Big Blue [*Jarrard*, 2003]. However, sediment may also act to insulate the incoming Pacific slab, allowing only conductive cooling of the slab in regions of thicker sediment cover rather than convective cooling through hydrothermal circulation [*Harris et al.*, 2010]. Altering the thermal state of the Pacific plate could delay or accelerate specific dehydration processes within the slab [*Spinelli and Wang*, 2009].

[48] The present-day Pacific slab subducting beneath the Mariana Islands is quite old, with many bathymetric highs and lows [*Stern and Smoot*, 1998; *Wessel*, 2001; *Stern et al.*, 2003; *Oakley et al.*,

2008]. Between ~16.5–17.75°N, the Mariana trench is deeper and the subducting Pacific plate has fewer seamounts; in the forearc west of this flat region and south of our observed earthquake clusters, thrust seismicity is notably scarce (Figures 5 and 6) [*Oakley et al.*, 2008]. The difference in the subducted seafloor along-strike is a compelling argument that the prominent seamounts subducted near 18°N is responsible for increased seismicity in the forearc of this region [*Tanioka et al.*, 1997; *Bilek*, 2007; *Oakley et al.*, 2008].

5.4. Mechanisms for Aseismic Slip in the Mariana Islands

[49] The results of this study show a clear concentration of small earthquakes along the plate interface, connecting results from *Oakley et al.* [2008] and the locations of shallow thrust GCMT solutions. While this indicates that the seismogenic zone is in fact larger than previously discussed [*Pacheco et al.*, 1993; *Hyndman*, 2007], the results also show that there are changes in the interplate seismogenic zone both along-strike and with depth. Our results show heterogeneity in the size of earthquakes along dip of the seismogenic zone and indicate depth-dependent segmentation of the fault into strong and weak regions. Additionally, our observation of clusters of small earthquakes occurring within the same region as found in 2001 by *Shiobara et al.* [2010] indicates that coupling of the seismogenic zone changes in the along-strike direction as well.

[50] Our observations that seismicity varies both with depth and along-strike of the Northern Mariana subduction zone imply a segmented and potentially less coupled seismogenic zone, but the exact cause of the observed variability remains uncertain. While recent tomographic results from the Mariana forearc suggest that partial serpentinization may contribute to our patterns of seismicity and quiescence [*Pozgay et al.*, 2009; *Barklage*, 2010; *Pyle et al.*, 2010], observations of seamounts subducting at the trench suggest that the cause may be related to the roughness of the subducting seafloor [*Oakley et al.*, 2008].

[51] We suggest that the observed variability is related to the mechanism responsible for presumed aseismic slip in Central and Northern Mariana. The variable seismogenic characteristics along-strike and with depth suggest that a single large locked region is not present along the Mariana subduction zone. Rather, the fault is likely creeping aseismically along portions of the interface, with stable sliding perhaps facilitated by the frictional characteristics of serpentine or by variable effective normal stresses at the plate interface. This heterogeneous character and prominence of stable sliding prohibits the formation of larger locked patches that could slip in great earthquakes, and leaves only disconnected small asperities capable of producing moderate-sized earthquakes.

6. Conclusions

[52] The key conclusion which can be drawn from this study is that the apparent limits of seismogenesis as revealed by earthquake locations and focal mechanisms indicate a shallow thrust zone that is ~100 km wide, extending from 20 to 60 km depth in the Northern Mariana Islands at 18°N near Big Blue Seamount. While past studies have suggested that the lack of large earthquakes in Mariana results from a shallow downdip limit of seismogenesis due to mantle serpentization, combined location inversions indicate that shallow thrust earthquakes found in the GCMT data set occur along with the locally recorded microearthquakes down to a depth of about 60 km. This result has a wide range of implications regarding seismogenesis along the plate interface in Northern Mariana. Furthermore, we suggest that observed patterns of seismicity indicate changes in coupling both along strike of the margin and with depth along the plate interface. This can be explained by multiple factors, such as subducted slab topography, expulsion of water from the slab, and formation of serpentinites within the mantle wedge. These mechanisms likely disrupt the continuance of coupling along-strike and affect the potential for nucleation of great, shallow thrust earthquakes in the Northern Mariana Islands.

Acknowledgments

[53] Many thanks to M. Barklage, H. Chou, G. Euler, D. Heeszel, S. Pozgay, M. Pyle, P. Shore, and S. Solomatov for their technical and scientific support. Special thanks to the scientists responsible for deployment and collection of the seismographs, including P. Shore, S. Webb, A. Sauter, H. Iwamoto, S. Pozgay, M. Barklage, B. Shiro, P. Jonke, J. Camacho, J. Kaipat, and R. Chong as well as the crew of the R/V Kaiyo, the R/V Wecoma, and the Super Emerald. Thanks to two anonymous reviewers and the associate editor whose attentive comments and suggestions improved this paper. Land seismometers were provided by the PASSCAL program of IRIS. Licensing for Antelope software was provided by IRIS. Research was funded by the MARGINS program of the National Science Foundation, under grants OCE-0001938 and EAR-0549056.

References

Abe, K. (1981), Magnitudes of large shallow earthquakes from 1904 to 1980, *Phys. Earth Planet. Inter.*, *27*(1), 72–92, doi:10.1016/0031-9201(81)90088-1.

Abe, K., and H. Kanamori (1979), Temporal variation of the activity of intermediate and deep focus earthquakes, *J. Geophys. Res.*, *84*(B7), 3589–3595, doi:10.1029/JB084iB07p03589.

Abe, K., and S. Noguchi (1983), Revision of magnitudes of large shallow earthquakes, 1897–1912, *Phys. Earth Planet. Inter.*, *33*(1), 1–11, doi:10.1016/0031-9201(83)90002-X.

Ammon, C. J., et al. (2005), Rupture process of the 2004 Sumatra-Andaman earthquake, *Science*, *308*(5725), 1133–1139, doi:10.1126/science.1112260.

Audet, P., M. G. Bostock, N. I. Christensen, and S. M. Peacock (2009), Seismic evidence for overpressured subducted oceanic crust and megathrust fault sealing, *Nature*, *457*(7225), 76–78, doi:10.1038/nature07650.

Barklage, M. (2010), Structure and seismicity of the upper mantle using deployments of broadband seismographs in Antarctica and the Mariana Islands, Ph.D. dissertation, 115 pp, Washington Univ. in Saint Louis, Saint Louis, Mo.

Benton, L. D., J. G. Ryan, and I. P. Savov (2004), Lithium abundance and isotope systematics of forearc serpentinites, Conical Seamount, Mariana forearc: Insights into the mechanics of slab-mantle exchange during subduction, *Geochem. Geophys. Geosyst.*, *5*, Q08J12, doi:10.1029/2004GC000708.

Bilek, S. L. (2007), Influence of subducting topography on earthquake rupture, in *The Seismogenic Zone of Subduction Thrust Faults*, edited by T. H. Dixon and J. C. Moore, pp. 123–146, Columbia Univ. Press, New York.

Bilek, S. L., and T. Lay (1999), Rigidity variations with depth along interplate megathrust faults in subduction zones, *Nature*, *400*(6743), 443–446, doi:10.1038/22739.

Bilek, S. L., and T. Lay (2000), Depth dependent rupture properties in Circum-Pacific subduction zones, in *Geocomplexity and the Physics of Earthquakes*, *Geophys. Monogr. Ser.*, vol. 120, edited by J. B. Rundle et al., pp. 165–186, AGU, Washington, D. C.

Bilek, S. L., S. Y. Schwartz, and H. R. DeShon (2003), Controls on seafloor roughness on earthquake rupture behavior, *Geology*, *31*(5), 455–458, doi:10.1130/0091-7613(2003)031<0455:COSROE>2.0.CO;2.

Byrne, D. E., D. M. Davis, and L. R. Sykes (1988), Loci and maximum size of thrust earthquakes and the mechanics of the shallow region of subduction zones, *Tectonics*, *7*(4), 833–857, doi:10.1029/TC007i004p00833.

Byrne, T., and D. Fisher (1990), Evidence for a weak and overpressured décollement beneath sediment-dominated accretionary prisms, *J. Geophys. Res.*, *95*(B6), 9081–9097, doi:10.1029/JB095iB06p09081.

Campos, J., R. Madariaga, and C. Scholz (1996), Faulting process of the August 8, 1993, Guam earthquake: A thrust event in an otherwise weakly coupled subduction zone, *J. Geophys. Res.*, *101*(B8), 17,581–17,596, doi:10.1029/96JB00654.

DeShon, H. R., S. Y. Schwartz, S. L. Bilek, L. M. Dorman, V. Gonzalez, J. M. Protti, E. R. Flueh, and T. H. Dixon (2003), Seismogenic zone structure of the southern Middle America Trench, Costa Rica, *J. Geophys. Res.*, *108*(B10), 2491, doi:10.1029/2002JB002294.

DeShon, H. R., S. Y. Schwartz, A. V. Newman, V. Gonzalez, M. Protti, L. M. Dorman, T. H. Dixon, D. E. Sampson, and E. R. Flueh (2006), Seismogenic zone structure beneath the Nicoya Peninsula, Costa Rica, from three-dimensional local earthquake P- and S-wave tomography, *Geophys. J. Int.*, *164*(1), 109–124, doi:10.1111/j.1365-246X.2005.02809.x.

Dziewonski, A. M., and D. L. Anderson (1981), Preliminary reference Earth model, *Phys. Earth Planet. Inter.*, *25*(4), 297–356, doi:10.1016/0031-9201(81)90046-7.

Dziewonski, A. M., T. A. Chou, and J. H. Woodhouse (1981), Determination of earthquake source parameters from waveform data for studies of global and regional seismicity, *J. Geophys. Res.*, *86*(B4), 2825–2852, doi:10.1029/JB086iB04p02825.

Freymueller, J. T., H. Woodard, S. C. Cohen, R. Cross, J. Elliott, C. F. Larsen, S. Hreinsdóttir, and C. Zweck (2008), Active deformation processes in Alaska, based on 15 years of GPS measurements, in *Active Tectonics and Seismic Potential of Alaska*, *Geophys. Monogr. Ser.*, vol. 179, edited by J. T. Freymueller et al., pp. 1–42, AGU, Washington, D. C.

Fryer, P. B., and M. H. Salisbury (2006), Leg 195 synthesis: Site 1200–Serpentinite seamounts of the Izu-Bonin/Mariana convergent plate margin (ODP Leg 125 and 195 drilling results), *Proc. Ocean Drill. Program Sci. Results*, *195*, 1–30, doi:10.2973/odp.proc.sr.195.112.2006.

Fryer, P., C. G. Wheat, and M. J. Mottl (1999), Mariana blueschist mud volcanism: Implications for conditions within the subduction zone, *Geology*, *27*(2), 103–106, doi:10.1130/0091-7613(1999)027<0103:MBMVIF>2.3.CO;2.

Fujita, K., E. R. Engdahl, and N. H. Sleep (1981), Subduction zone calibration and teleseismic relocation of thrust zone events in the central Aleutian Islands, *Bull. Seismol. Soc. Am.*, *71*(6), 1805–1828.

Gardner, J. V. (2010), U.S. Law of the Sea cruises to map sections of the Mariana Trench and the eastern and southern insular margins of Guam and the Northern Mariana Islands, UNH-CCOM/JHC Tech. Rep. 10–003, Cent. for Coastal and Ocean Mapp. Joint Hydrographic Cent, Durham, N. C.

Ghosh, A., A. V. Newman, A. M. Thomas, and G. T. Farmer (2008), Interface locking along the subduction megathrust from b-value mapping near Nicoya Peninsula, Costa Rica, *Geophys. Res. Lett.*, *35*, L01301, doi:10.1029/2007GL031617.

Gutenberg, B. (1956), Great earthquakes 1896–1903, *Eos Trans. AGU*, *37*(5), 608–614.

Gutenberg, B., and C. F. Richter (1954), *Seismicity of the Earth and Associated Phenomena*, 2nd ed., Hafner, New York.

Hacker, B. R. (2008), H_2O subduction beyond arcs, *Geochem. Geophys. Geosyst.*, *9*, Q03001, doi:10.1029/2007GC001707.

Hacker, B. R., G. A. Abers, and S. M. Peacock (2003), Subduction factory: 1. Theoretical mineralogy, densities, seismic wave speeds, and H_2O contents, *J. Geophys. Res.*, *108*(B1), 2029, doi:10.1029/2001JB001127.

Hall, R. (2002), Cenozoic geological and plate tectonic evolution of SE Asia and the SW Pacific: Computer-based reconstructions, model and animations, *J. Asian Earth Sci.*, *20*(4), 353–431, doi:10.1016/S1367-9120(01)00069-4.

Hall, R., J. R. Ali, C. D. Anderson, and S. J. Baker (1995), Origin and motion history of the Philippine Sea Plate, *Tectonophysics*, *251*(1–4), 229–250, doi:10.1016/0040-1951(95)00038-0.

Harada, T., and K. Ishibashi (2008), Interpretation of the 1993, 2001, and 2002 Guam earthquakes as intraslab events by a simultaneous relocation of the mainshocks, aftershocks, and background earthquakes, *Bull. Seismol. Soc. Am.*, *98*(3), 1581–1587, doi:10.1785/0120060227.

Harris, R. N., and K. Wang (2002), Thermal models of the middle America trench at the Nicoya Peninsula, Costa Rica, *Geophys. Res. Lett.*, *29*(21), 2010, doi:10.1029/2002GL015406.

Harris, R. N., G. Spinelli, C. R. Ranero, I. Grevemeyer, H. Villinger, and U. Barckhausen (2010), Thermal regime of the Costa Rican convergent margin: 2. Thermal models of the shallow Middle America subduction zone offshore Costa Rica, *Geochem. Geophys. Geosyst.*, *11*, Q12S29, doi:10.1029/2010GC003273.

Hasegawa, A., N. Uchida, T. Igarashi, T. Matsuzawa, T. Okada, S. Miura, and Y. Suwa (2007), Asperities and quasi-static slips on the subducting plate boundary east of Tohoku, Northeast Japan, in *The Seismogenic Zone of Subduction Thrust Faults*, edited by T. H. Dixon and J. C. Moore, pp. 451–475, Columbia Univ. Press, New York.

Hilairet, N., B. Reynard, Y. B. Wang, I. Daniel, S. Merkel, N. Nishiyama, and S. Petitgirard (2007), High-pressure creep of serpentine, interseismic deformation, and initiation of subduction, *Science*, *318*(5858), 1910–1913, doi:10.1126/science.1148494.

Hulme, S. M., C. G. Wheat, P. Fryer, and M. J. Mottl (2010), Pore water chemistry of the Mariana serpentinite mud volcanoes: A window to the seismogenic zone, *Geochem. Geophys. Geosyst.*, *11*, Q01X09, doi:10.1029/2009GC002674.

Hyndman, R. D. (2007), What we know and don't know, in *The Seismogenic Zone of Subduction Thrust Faults*, edited by T. H. Dixon and J. C. Moore, pp. 15–40, Columbia Univ. Press, New York.

Hyndman, R. D., and K. Wang (1993), Thermal constraints on the zone of major thrust earthquake failure: The Cascadia subduction zone, *J. Geophys. Res.*, *98*(B2), 2039–2060, doi:10.1029/92JB02279.

Hyndman, R. D., K. Wang, and M. Yamano (1995), Thermal constraints on the seismogenic portion of the southwestern Japan subduction thrust, *J. Geophys. Res.*, *100*(B8), 15,373–15,392, doi:10.1029/95JB00153.

Hyndman, R. D., M. Yamano, and D. A. Oleskevich (1997), The seismogenic zone of subduction thrust faults, *Isl. Arc*, *6*(3), 244–260, doi:10.1111/j.1440-1738.1997.tb00175.x.

Igarashi, T., T. Matsuzawa, N. Umino, and A. Hasegawa (2001), Spatial distribution of focal mechanisms for interplate and intraplate earthquakes associated with the subducting Pacific plate beneath the northeastern Japan arc: A triple-planed deep seismic zone, *J. Geophys. Res.*, *106*(B2), 2,177–2,191, doi:10.1029/2000JB900386.

Jarrard, R. D. (2003), Subduction fluxes of water, carbon dioxide, chlorine, and potassium, *Geochem. Geophys. Geosyst.*, *4*(5), 8905, doi:10.1029/2002GC000392.

Jordan, T. H., and K. A. Sverdrup (1981), Teleseismic location techniques and their application to earthquake clusters in the South-Central Pacific, *Bull. Seismol. Soc. Am.*, *71*(4), 1105–1130.

Kanamori, H. (1977), Seismic and aseismic slip along subduction zones and their tectonic implications, in *Island Arcs Deep Sea Trenches and Back-Arc Basins*, *Maurice Ewing Ser.*, vol. 1, edited by M. Talwani and W. C. Pitman III, pp. 163–174, AGU, Washington, D. C.

Kato, T., J. Beavan, T. Matsushima, Y. Kotake, J. T. Camacho, and S. Nakao (2003), Geodetic evidence of back-arc spreading in the Mariana Trough, *Geophys. Res. Lett.*, *30*(12), 1625, doi:10.1029/2002GL016757.

Keating, B. H., D. P. Mattey, C. E. Helsley, J. J. Naughton, D. Epp, A. Lazarewicz, and D. Schwank (1984), Evidence for a hot spot origin of the Caroline Islands, *J. Geophys. Res.*, *89*(B12), 9937–9948, doi:10.1029/JB089iB12p09937.

Kennett, B. L. N. (1983), *Seismic Wave Propagation in Stratified Media*, 339 pp., Cambridge Univ. Press, Cambridge, U. K.

Kennett, B. L. N., and E. R. Engdahl (1991), Traveltimes for global earthquake location and phase identification, *Geophys. J. Int.*, *105*(2), 429–465, doi:10.1111/j.1365-246X.1991.tb06724.x.

Langston, C. A., and D. V. Helmberger (1975), A procedure for modeling shallow dislocation sources, *Geophys. J. R. Astron. Soc.*, *42*(1), 117–130, doi:10.1111/j.1365-246X.1975.tb05854.x.

Lay, T., et al. (2005), The great Sumatra-Andaman earthquake of 26 December 2004, *Science*, *308*(5725), 1127–1133, doi:10.1126/science.1112250.

Marone, C., and C. H. Scholz (1988), The depth of seismic faulting and the upper transition from stable to unstable slip regimes, *Geophys. Res. Lett.*, *15*(6), 621–624, doi:10.1029/GL015i006p00621.

Maso, M. S. (1910), *Catalogue of Violent and Destructive Earthquakes in the Philippines, with an Appendix, Earthquakes in the Marianas Islands; 1599–1909*, Philipp. Isl. Weather Bur., Manila.

Moore, D. E., and D. A. Lockner (2007), Comparative deformation behavior of minerals in serpentinized ultramafic rock: Application to the slab-mantle interface in subduction zones, *Int. Geol. Rev.*, *49*(5), 401–415, doi:10.2747/0020-6814.49.5.401.

Moore, D. E., D. A. Lockner, S. L. Ma, R. Summers, and J. D. Byerlee (1997), Strengths of serpentinite gouges at elevated temperatures, *J. Geophys. Res.*, *102*(B7), 14,787–14,801, doi:10.1029/97JB00995.

Moore, J. C., and D. M. Saffer (2001), Updip limit of the seismogenic zone beneath the accretionary prism of southwest Japan: An effect of diagenetic to low-grade metamorphic processes and increasing effective stress, *Geology*, *29*(2), 183–186, doi:10.1130/0091-7613(2001)029<0183:ULOTSZ>2.0.CO;2.

Newman, A. V., S. Y. Schwartz, V. Gonzalez, H. R. DeShon, J. M. Protti, and L. M. Dorman (2002), Along-strike variability in the seismogenic zone below Nicoya Peninsula, Costa Rica, *Geophys. Res. Lett.*, *29*(20), 1977, doi:10.1029/2002GL015409.

Norabuena, E., et al. (2004), Geodetic and seismic constraints on some seismogenic zone processes in Costa Rica, *J. Geophys. Res.*, *109*, B11403, doi:10.1029/2003JB002931.

Oakley, A. J., B. Taylor, P. Fryer, G. E. Moore, A. M. Goodliffe, and J. K. Morgan (2007), Emplacement, growth, and gravitational deformation of serpentinite seamounts on the Mariana forearc, *Geophys. J. Int.*, *170*(2), 615–634, doi:10.1111/j.1365-246X.2007.03451.x.

Oakley, A. J., B. Taylor, and G. F. Moore (2008), Pacific Plate subduction beneath the central Mariana and Izu-Bonin fore arcs: New insights from an old margin, *Geochem. Geophys. Geosyst.*, *9*, Q06003, doi:10.1029/2007GC001820.

Oleskevich, D. A., R. D. Hyndman, and K. Wang (1999), The updip and downdip limits to great subduction earthquakes: Thermal and structural models of Cascadia, south Alaska, SW Japan, and Chile, *J. Geophys. Res.*, *104*(B7), 14,965–14,991, doi:10.1029/1999JB900060.

Pacheco, J. F., and L. R. Sykes (1992), Seismic moment catalog of large shallow earthquakes, 1900 to 1989, *Bull. Seismol. Soc. Am.*, *82*(3), 1306–1349.

Pacheco, J. F., L. R. Sykes, and C. H. Scholz (1993), Nature of seismic coupling along simple plate boundaries of the subduction type, *J. Geophys. Res.*, *98*(B8), 14,133–14,159, doi:10.1029/93JB00349.

Pavlis, G. L., F. Vernon, D. Harvey, and D. Quinlan (2004), The generalized earthquake-location (GENLOC) package: An earthquake-location library, *Comput. Geosci.*, *30*(9–10), 1079–1091, doi:10.1016/j.cageo.2004.06.010.

Peacock, S. M., and R. D. Hyndman (1999), Hydrous minerals in the mantle wedge and the maximum depth of subduction thrust earthquakes, *Geophys. Res. Lett.*, *26*(16), 2517–2520, doi:10.1029/1999GL900558.

Pozgay, S. H., R. A. White, D. A. Wiens, P. J. Shore, A. W. Sauter, and J. L. Kaipat (2005), Seismicity and tilt associated with the 2003 Anatahan eruption sequence, *J. Volcanol. Geotherm. Res.*, *146*(1–3), 60–76, doi:10.1016/j.jvolgeores.2004.12.008.

Pozgay, S. H., D. A. Wiens, J. A. Conder, H. Shiobara, and H. Sugioka (2007), Complex mantle flow in the Mariana subduction system: Evidence from shear wave splitting, *Geophys. J. Int.*, *170*(1), 371–386, doi:10.1111/j.1365-246X.2007.03433.x.

Pozgay, S., D. A. Wiens, J. A. Conder, H. Shiobara, and H. Sugioka (2009), Seismic attenuation tomography of the Mariana arc: Implications for thermal structure, volatile distribution, and dynamics, *Geochem. Geophys. Geosyst.*, *10*, Q04X05, doi:10.1029/2008GC002313.

Pyle, M., D. A. Wiens, D. S. Weeraratne, P. J. Shore, H. Shiobara, and H. Sugioka (2010), Shear velocity structure of the Mariana mantle wedge from Rayleigh wave phase velocities, *J. Geophys. Res.*, *115*, B11304, doi:10.1029/2009JB006976.

Reinen, L. A., J. D. Weeks, and T. E. Tullis (1991), The frictional behavior of serpentinite - Implications for aseismic creep on shallow crustal faults, *Geophys. Res. Lett.*, *18*(10), 1921–1924, doi:10.1029/91GL02367.

Richter, C. F. (1958), *Elementary Seismology*, W. H. Freeman, San Francisco, Calif.

Rossi, G., G. A. Abers, S. Rondenay, and D. H. Christensen (2006), Unusual mantle Poisson's ratio, subduction, and crustal structure in central Alaska, *J. Geophys. Res.*, *111*, B09311, doi:10.1029/2005JB003956.

Saffer, D. M., and C. Marone (2003), Comparison of smectite- and illite-rich gouge frictional properties: Application to the updip limit of the seismogenic zone along subduction megathrusts, *Earth Planet. Sci. Lett.*, *215*(1–2), 219–235, doi:10.1016/S0012-821X(03)00424-2.

Satake, K., Y. Yoshida, and K. Abe (1992), Tsunami from the Mariana earthquake of April 5, 1990–its abnormal propagation and implications for tsunami potential from outer-rise earthquakes, *Geophys. Res. Lett.*, *19*(3), 301–304, doi:10.1029/91GL02493.

Scholz, C. H., and J. Campos (1995), On the mechanism of seismic decoupling and back arc spreading at subduction zones, *J. Geophys. Res.*, *100*(B11), 22,103–22,115, doi:10.1029/95JB01869.

Schwartz, S. Y., and H. R. DeShon (2007), Distinct updip limits to geodetic locking and microseismicity at the northern Costa Rica seismogenic zone: Evidence for two mechanical transitions, in *The Seismogenic Zone of Subduction Thrust Faults*, edited by T. H. Dixon and J. C. Moore, pp. 576–599, Columbia Univ. Press, New York.

Seno, T. (2005), Variation of downdip limit of the seismogenic zone near the Japanese islands: Implications for the serpentinization mechanism of the forearc mantle wedge, *Earth Planet. Sci. Lett.*, *231*(3–4), 249–262, doi:10.1016/j.epsl.2004.12.027.

Shelly, D. R., G. C. Beroza, S. Ide, and S. Nakamula (2006), Low-frequency earthquakes in Shikoku, Japan, and their relationship to episodic tremor and slip, *Nature*, *442*(7099), 188–191, doi:10.1038/nature04931.

Shinohara, M., R. Hino, T. Yoshizawa, M. Nishino, T. Sato, and K. Suyehiro (2005), Hypocenter distribution of plate boundary zone off Fukushima, Japan, derived from ocean bottom seismometer data, *Earth Planets Space*, *57*(2), 93–105.

Shiobara, H., H. Sugioka, K. Mochizuki, S. Oki, T. Kanazawa, Y. Fukao, and K. Suyehiro (2010), Double seismic zone in the North Mariana region revealed by long-term ocean bottom array observation, *Geophys. J. Int.*, *183*(3), 1455–1469, doi:10.1111/j.1365-246X.2010.04799.x.

Smith, W. H. F., H. Staudigel, A. B. Watts, and M. S. Pringle (1989), The Magellan seamounts: Early Cretaceous record of the South Pacific isotopic and thermal anomaly, *J. Geophys. Res.*, *94*(B8), 10,501–10,523, doi:10.1029/JB094iB08p10501.

Snoke, J. A., J. W. Munsey, A. C. Teague, and G. A. Bollinger (1984), A program for focal mechanism determination by combined use of polarity and SV-P amplitude ratio data, *Earthquake Notes*, *55*, 15.

Soloviev, S. L., and C. N. Go (1974), *A Catalogue of Tsunamis on the Western Shore of the Pacific Ocean* [in Russian], Nauka, Moscow. [English translation, *Can. Transl. Fish Aquat. Sci.*, vol. 5077, 447 pp., Inst. Ocean Sci., Sidney, B. C., Canada, 1984].

Spinelli, G. A., and D. M. Saffer (2004), Along-strike variations in underthrust sediment dewatering on the Nicoya margin, Costa Rica related to the updip limit of seismicity, *Geophys. Res. Lett.*, *31*, L04613, doi:10.1029/2003GL018863.

Spinelli, G. A., and K. Wang (2009), Links between fluid circulation, temperature, and metamorphism in subducting slabs, *Geophys. Res. Lett.*, *36*, L13302, doi:10.1029/2009GL038706.

Stern, R. J., and N. C. Smoot (1998), A bathymetric overview of the Mariana forearc, *Isl. Arc*, *7*(3), 525–540, doi:10.1111/j.1440-1738.1998.00208.x.

Stern, R. J., M. J. Fouch, and S. L. Klemperer (2003), An overview of the Izu-Bonin-Mariana subduction factory, in *Inside the Subduction Factory*, *Geophys. Monogr. Ser.*, vol. 138, edited by J. M. Eiler, pp. 175–222, AGU, Washington, D. C.

Takahashi, N., S. Kodaira, S. L. Klemperer, Y. Tatsumi, Y. Kaneda, and K. Suyehiro (2007), Crustal structure and evolution of the Mariana intra-oceanic island arc, *Geology*, *35*(3), 203–206, doi:10.1130/G23212A.1.

Tanioka, Y., K. Satake, and L. Ruff (1995), Analysis of seismological and tsunami data from the 1993 Guam Earthquake, *Pure Appl. Geophys.*, *144*(3–4), 823–837, doi:10.1007/BF00874396.

Tanioka, Y., L. Ruff, and K. Satake (1997), What controls the lateral variation of large earthquake occurrence along the Japan Trench?, *Isl. Arc*, *6*(3), 261–266, doi:10.1111/j.1440-1738.1997.tb00176.x.

Tibi, R., D. A. Wiens, and X. H. Yuan (2008), Seismic evidence for widespread serpentinized forearc mantle along the Mariana convergent margin, *Geophys. Res. Lett.*, *35*, L13303, doi:10.1029/2008GL034163.

Tichelaar, B. W., and L. J. Ruff (1993), Depth of seismic coupling along subduction zones, *J. Geophys. Res.*, *98*(B2), 2017–2037, doi:10.1029/92JB02045.

Uyeda, S., and H. Kanamori (1979), Back-arc opening and the mode of subduction, *J. Geophys. Res.*, *84*(B3), 1049–1061, doi:10.1029/JB084iB03p01049.

Vrolijk, P. (1990), On the mechanical role of smectite in subduction zones, *Geology*, *18*(8), 703–707, doi:10.1130/0091-7613(1990)018<0703:OTMROS>2.3.CO;2.

Wada, I., and K. L. Wang (2009), Common depth of slab-mantle decoupling: Reconciling diversity and uniformity of subduction zones, *Geochem. Geophys. Geosyst.*, *10*, Q10009, doi:10.1029/2009GC002570.

Webb, S. C., T. K. Deaton, and J. C. Lemire (2001), A broadband ocean-bottom seismometer system based on a 1-Hz

natural period geophone, *Bull. Seismol. Soc. Am.*, *91*(2), 304–312, doi:10.1785/0120000110.

Wessel, P. (2001), Global distribution of seamounts inferred from gridded Geosat/ERS-1 altimetry, *J. Geophys. Res.*, *106*(B9), 19,431–19,441, doi:10.1029/2000JB000083.

Yamamoto, Y., et al. (2008), Spatial heterogeneity of the mantle wedge structure and interplate coupling in the NE Japan forearc region, *Geophys. Res. Lett.*, *35*, L23304, doi:10.1029/2008GL036100.

Yamanaka, Y., and M. Kikuchi (2004), Asperity map along the subduction zone in northeastern Japan inferred from regional seismic data, *J. Geophys. Res.*, *109*, B07307, doi:10.1029/2003JB002683.

Yoshida, Y., K. Satake, and K. Abe (1992), The large normal-faulting Mariana earthquake of April 5, 1990 in uncoupled subduction zone, *Geophys. Res. Lett.*, *19*(3), 297–300, doi:10.1029/92GL00165.